Lecture 5: Solid Earth loading: Applications

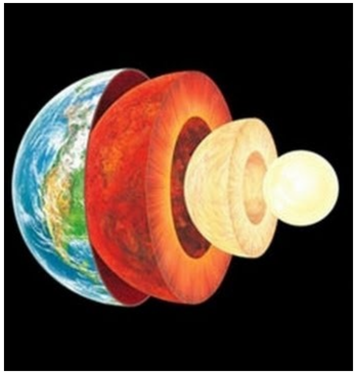

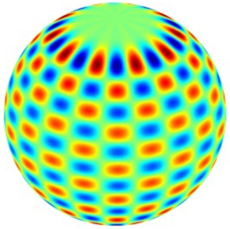

Makan Karegar
June 22, 2023
karegar@uni-bonn.de

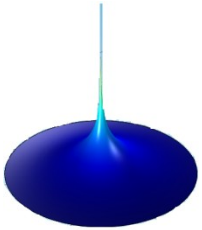

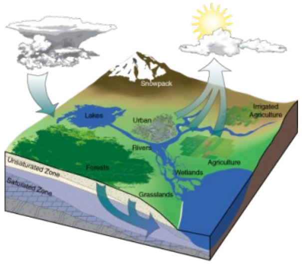

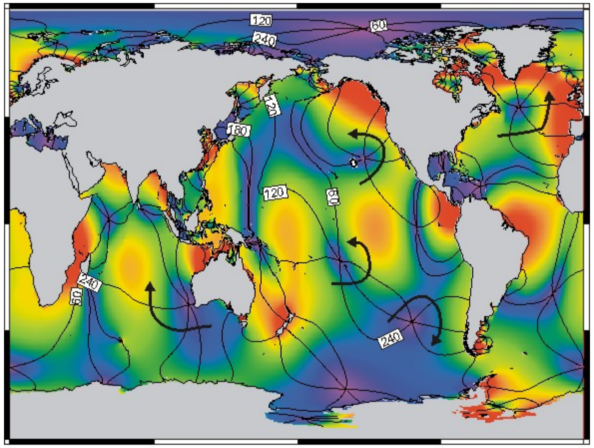

Tidal and non-tidal ocean loading

Tidal and non-tidal atmospheric loading

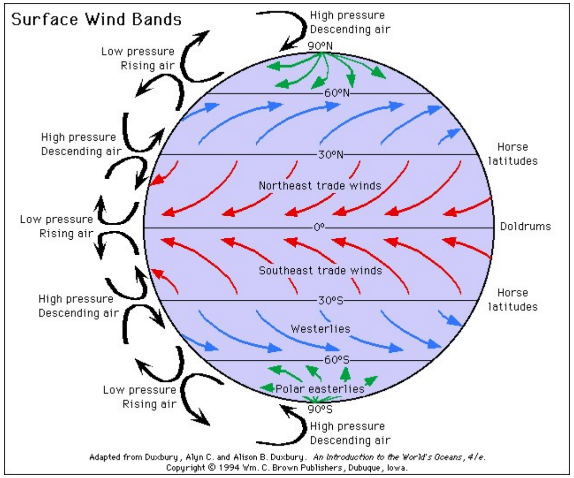

Hydrological loading

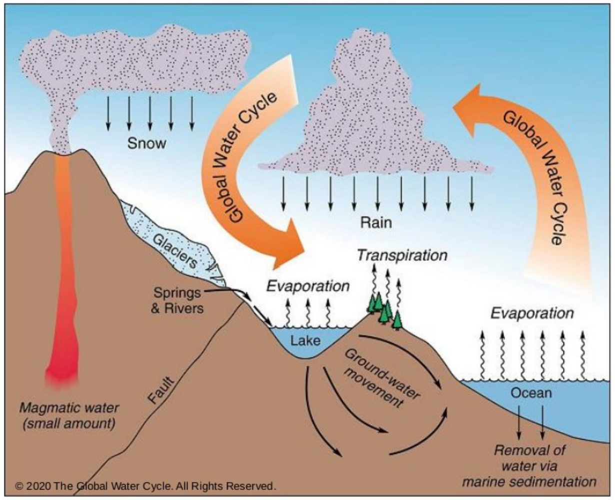

Cryospheric loading

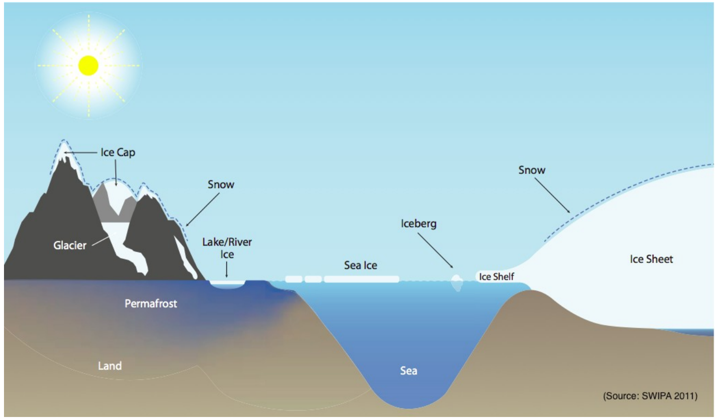

Loading: corrections for geodetic data and/or a process to study Earth's structure and underlying processes

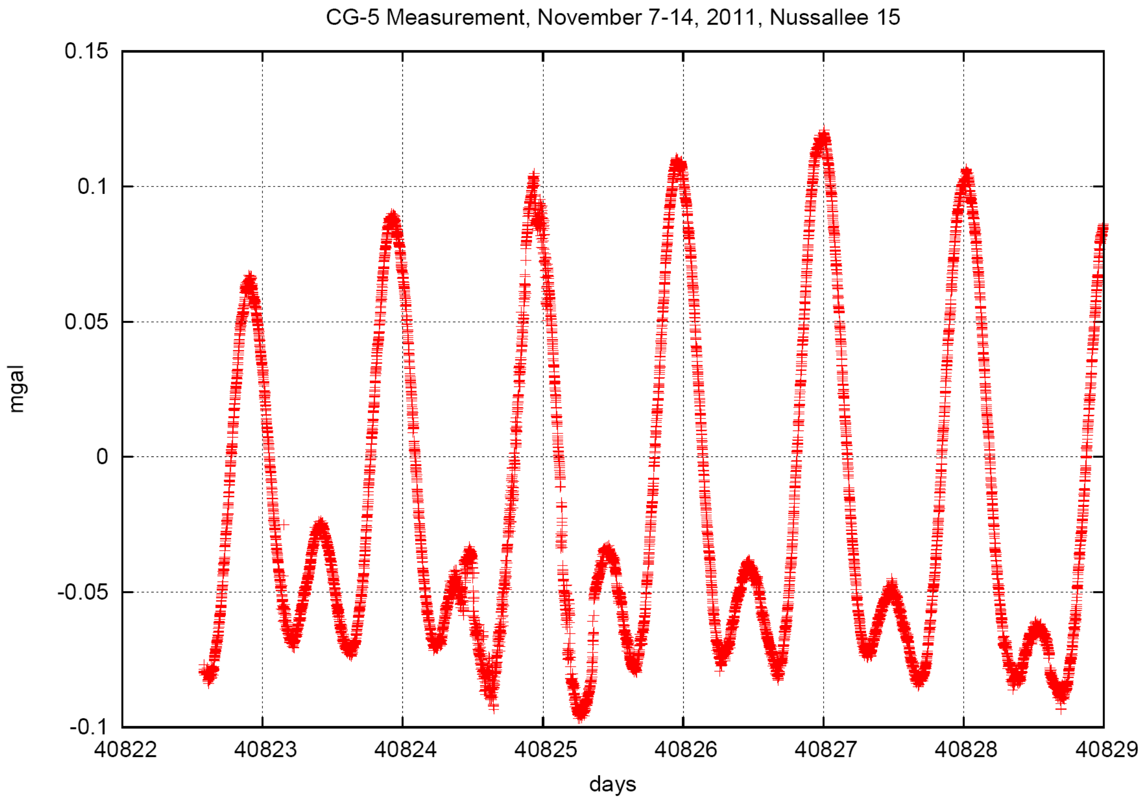

Objectives:

1. **Reduction (correction) of geodetic observations for studying a specific process – e.g. correcting GPS time series to find deformations due to tectonics, volcano, slow-slip ans etc.**

2. **Understanding processes (e.g. ocean) from observations, which include the response of the solid Earth (indirect Effects)**

3. **Better understanding of the Earth structure, through improving Earth models from observations**

Use of Earth models in geodesy

Elastic Models
- homogeneous solutions of the PDEs >> Love numbers
- Earth tides
- Loading >> mass transports within the Earth system
    - Atmospheric loading / gravitation of the atmospheric masses
    - Ocean tides / ocean load tides
    - non-tidal ocean mass change (e.g. changes in currents, sea level change)
    - Snow/ice accumulation and melting / polar regions
    - Water storage variability (groundwater, surface water, …)

Anelastic models
- In reality, Earth tides follow the tide-generating body slightly delayed (i.e. with a small lag time or angle). Another example: Post-seismic deformation

Viscoelastic models (similar to Anelastic models but much longer time scale)
- Postglacial rebound / GIA, Earthquake modeling (post-seismic deformation)

Poroelastic models
- Earthquake geodesy, tectonics, aquifer compaction

Forward model vs. Inverse model

Forward model:

$$v(\theta, \lambda, t) = a^2 \iint_\sigma \Delta\sigma(\theta', \lambda', t)\ G(\psi)\ d\sigma$$

From mass to displacement

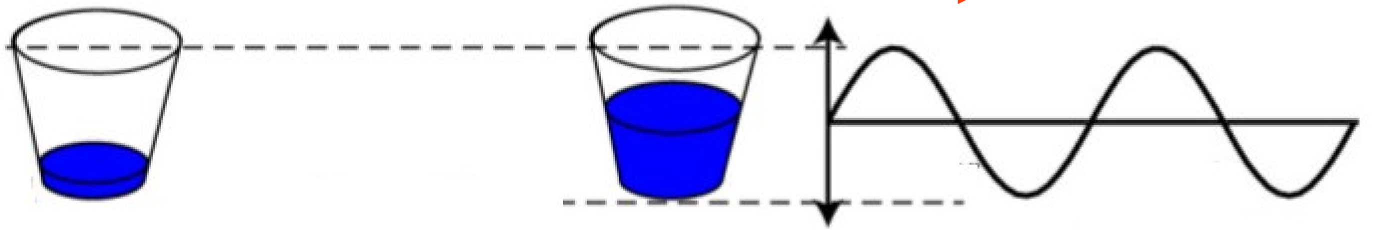

Inverse model:

From displacement to mass

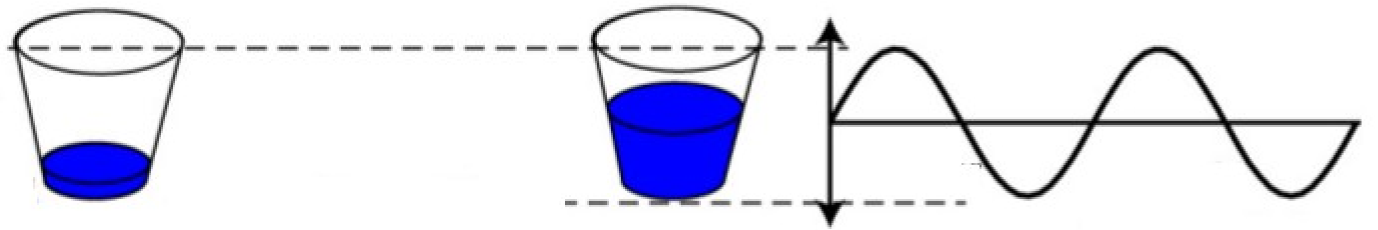

$$(\mathbf{Ax} - \mathbf{b})/\boldsymbol{\sigma})^2 + \beta^2 (L(\mathbf{x}))^2$$

B: vector of GPS observations of the seasonal vertical oscillation, **σ:** the vector of standard errors,
X: vector of surface water mass at each pixel, **A:** design matrix consisting of the Green's functions
L: Laplacian operator, β: a regularization factor

Your data

Annual variation

$$u(t_i) = a + vt_i + c\,sin(2\pi t_i) + d\,cos(2\pi t_i) + e\,sin(4\pi t_i) + f\,cos(4\pi t_i)$$

Linear trend

Semi-annual variation

Model parameters are calculated using LSQ.

Alternatively, the RMS scatter of time series around a linear term is use to demonstrate variability of loading data.

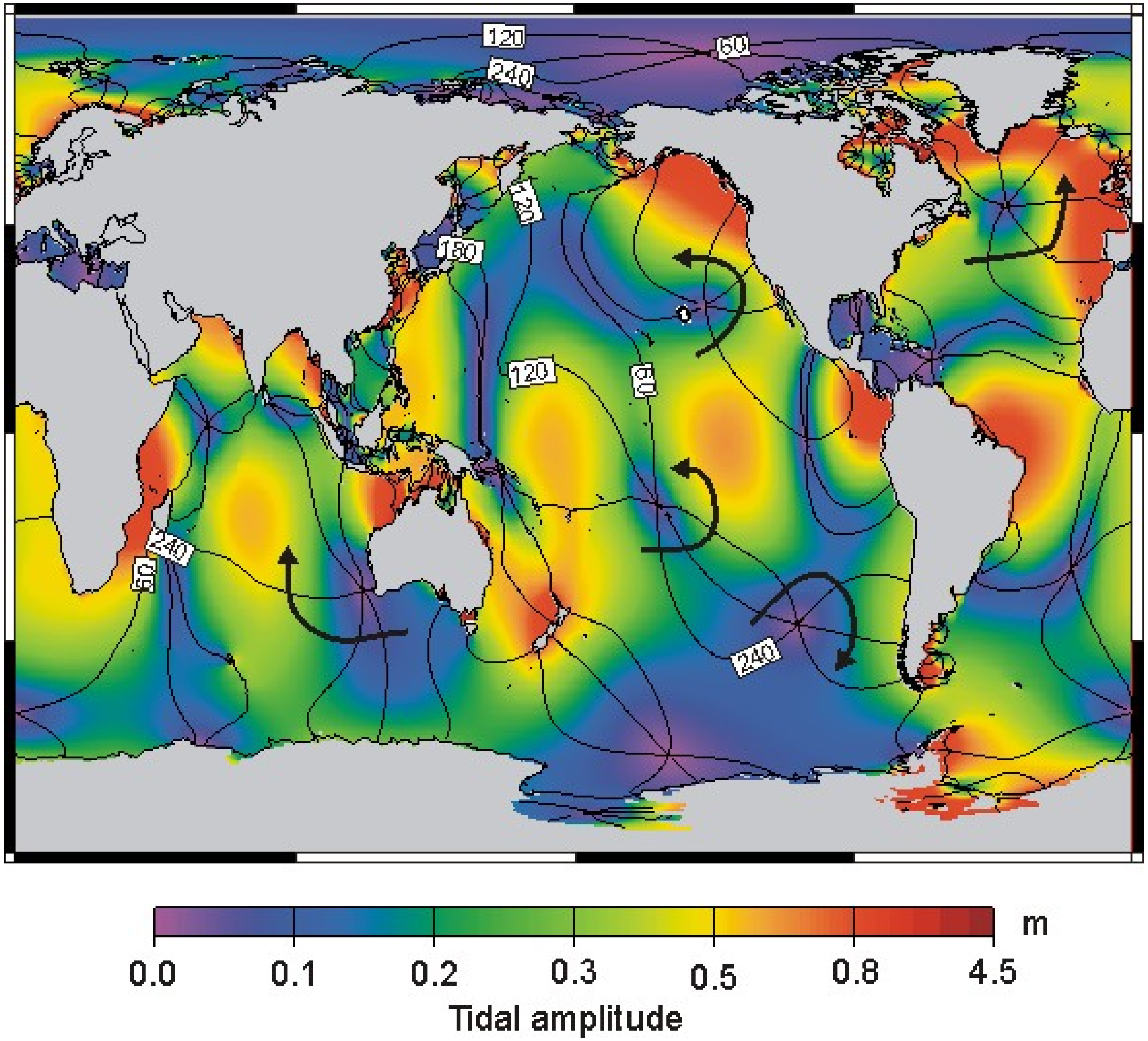

The ocean tides for harmonic M2

OTL provider: *http://holt.oso.chalmers.se/loading/*
Gives you displacement for specific lat/long

Tidal ocean loading

```
$$ Ocean loading displacement
$$
$$ OTL provider: http://holt.oso.chalmers.se/loading/
$$ Created by Scherneck & Bos
$$
$$ COLUMN ORDER:  M2  S2  N2  K2  K1  O1  P1  Q1  MF  MM SSA
$$
$$ ROW ORDER:
$$ AMPLITUDES (m)
$$   RADIAL
$$   TANGENTL    EW
$$   TANGENTL    NS
$$ PHASES (degrees)
$$   RADIAL
$$   TANGENTL    EW
$$   TANGENTL    NS
$$
$$ Displacement is defined positive in upwards, South and West direction.
$$ The phase lag is relative to Greenwich and lags positive. The PREM
$$ Green's function is used. The deficit of tidal water mass in the tide
$$ model has been corrected by subtracting a uniform layer of water with
$$ a certain phase lag globally.
$$
$$ CMC:  NO (corr.tide centre of mass)
$$
$$ TPXO.9_atl: m2 s2 n2 k2 k1 o1 p1 q1
$$ FES2012_comp: Mf Mm Ssa
$$
$$ END HEADER
$$
  MGW1
$$ TPXO9 ID:2020-05-10 12:32:01
$$ Computed using CARGA at SEGAL (UBI/IDL)
$$ MGW1                     RADI TANG  lon/lat: 270.0535   29.6185     1.471
  .00394 .00134 .00059 .00037 .00082 .00051 .00025 .00014 .00046 .00021 .00015
  .00168 .00050 .00038 .00015 .00084 .00063 .00027 .00013 .00007 .00002 .00001
  .00105 .00009 .00030 .00002 .00091 .00073 .00029 .00015 .00005 .00002 .00002
   117.2 -178.8   88.6 -171.8  -55.0 -120.9  -53.1  163.4 -180.0  176.7  174.6
   176.1  168.6  154.5  163.3 -151.9 -178.8 -157.4  170.7  135.1   96.3   21.0
  -157.6 -168.3  171.6  175.0   36.0   14.7   33.5   -9.3   -2.8  -18.4    2.9
```

Non-tidal ocean loading or ocean bottom pressure loading

DOI 10.1007/s00190-012-0564-5

ORIGINAL ARTICLE

Nontidal ocean loading: amplitudes and potential effects in GPS height time series

T. van Dam · X. Collilieux · J. Wuite · Z. Altamimi · J. Ray

Received: 21 February 2011 / Accepted: 10 April 2012

Abstract Ocean bottom pressure (OBP) changes are caused by a redistribution of the ocean's internal mass that are driven by atmospheric circulation, a change in the mass entering or leaving the ocean, and/or a change in the integrated atmospheric mass over the ocean areas. The only previous global analysis investigating the magnitude of OBP surface displacements used older OBP data sets (van Dam et al. in J Geophys Res 129:507–517, 1997). Since then significant improvements in meteorological forcing models used to predict OBP have been made, augmented by observations from satellite altimetry and expendable bathythermograph profiles. Using more recent OBP estimates from the Estimating the Circulation and Climate of the Ocean (ECCO) project, we reassess the amplitude of the predicted effect of OBP on the height coordinate time series from a global distribution effect of OBP on GPS height coordinate time series using the MIT reprocessed solution, mi1. When we compare the predicted OBP height time series with mi1, we find that the scatter is reduced over all stations by 0.1 mm on average with reductions as high as 0.7 mm at some stations. More importantly we are able to reduce the scatter on 65 % of the stations investigated. The annual component of the OBP signal is responsible for 80 % of the reduction in scatter on average. We find that stations located close to semi-enclosed bays or seas are affected by OBP loading to a greater extent than other stations.

Keywords Loading effects · Ocean bottom pressure · Height coordinate time series · Annual signals

RMS of variability of predicted ocean bottom pressure height displacements for every 2.5 degree

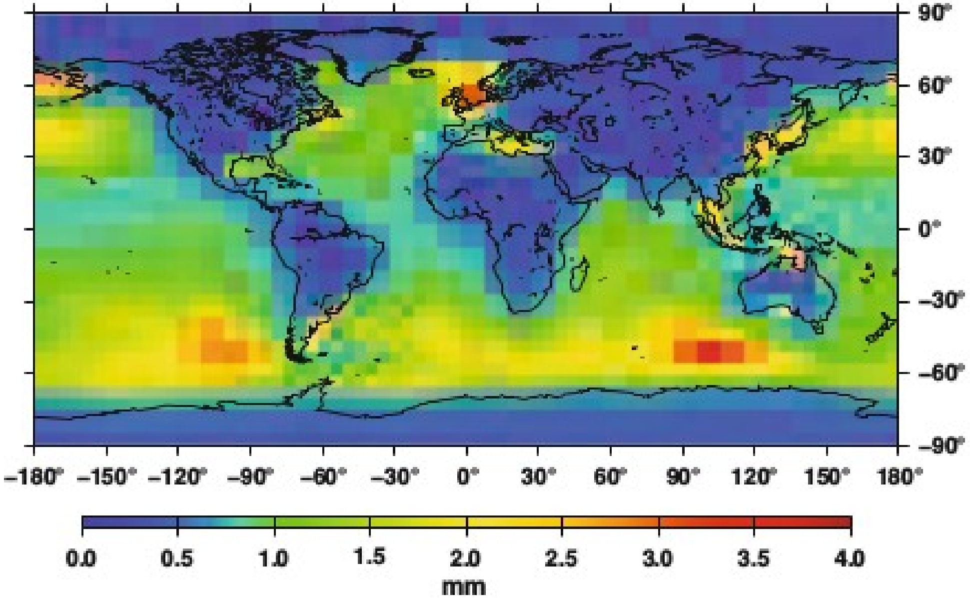

Maximum predicted surface displacement

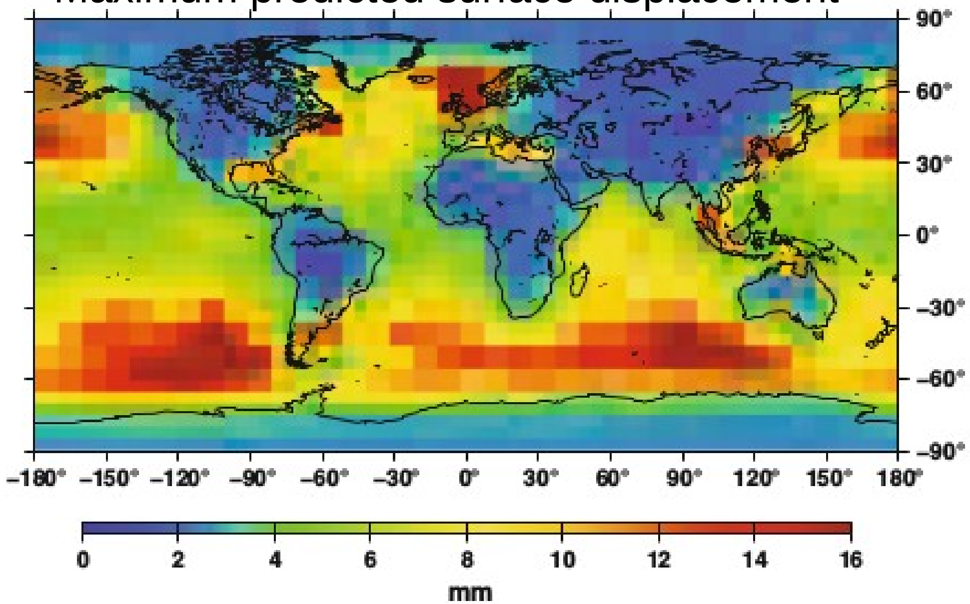

What caused ocean bottom pressure change?

1) **Water mass flux: Evaporation and Precipitation, Ice melt, river discharge**
2) **Ocean circulation**
3) **Atmospheric pressure change over ocean (inverse barometric (IB) effect)**

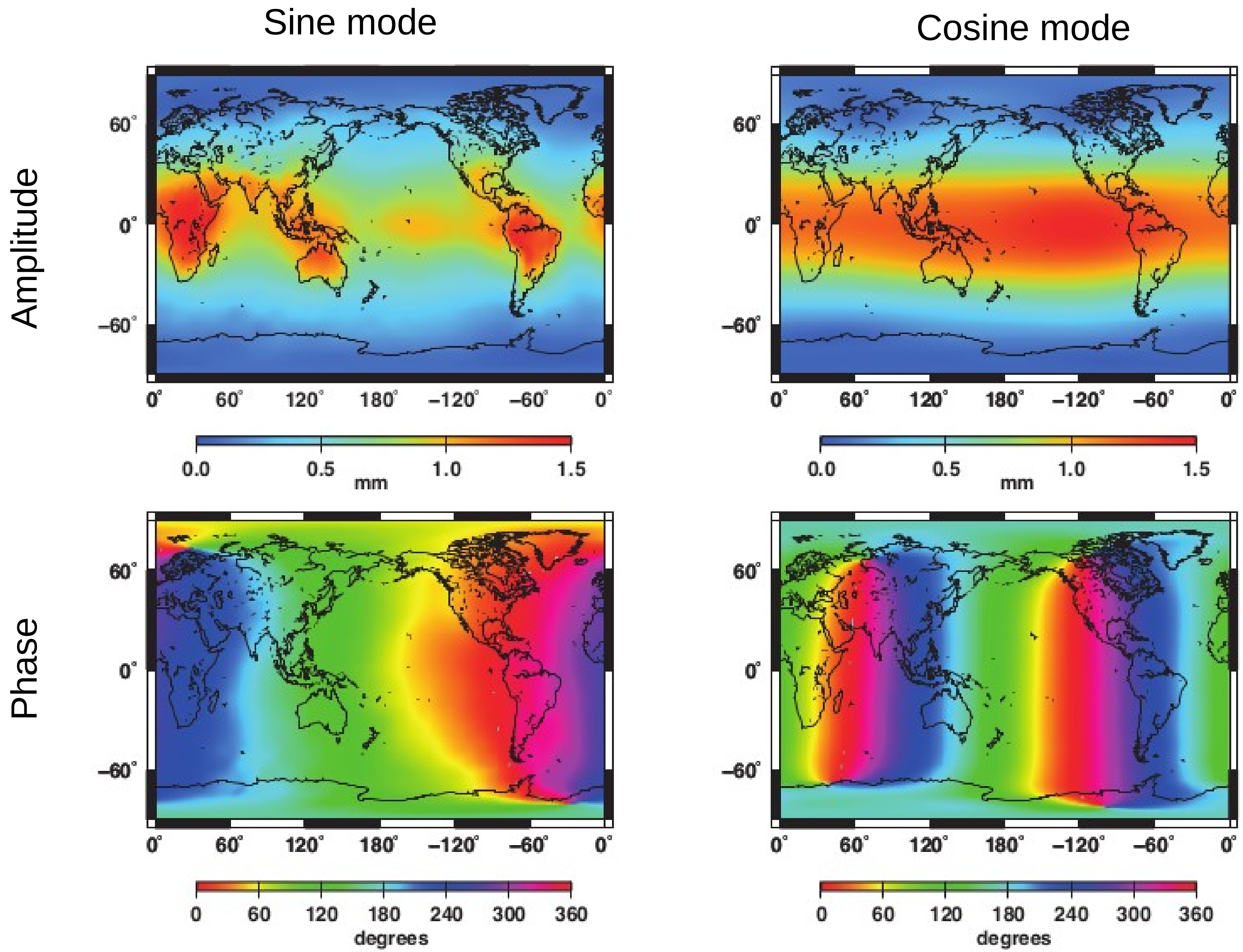

van Dam & Ray (2010) S1 and S2 Atmospheric Tide Loading Effects for Geodetic Applications

National Centers for Environmental Prediction (NCEP) pressure data

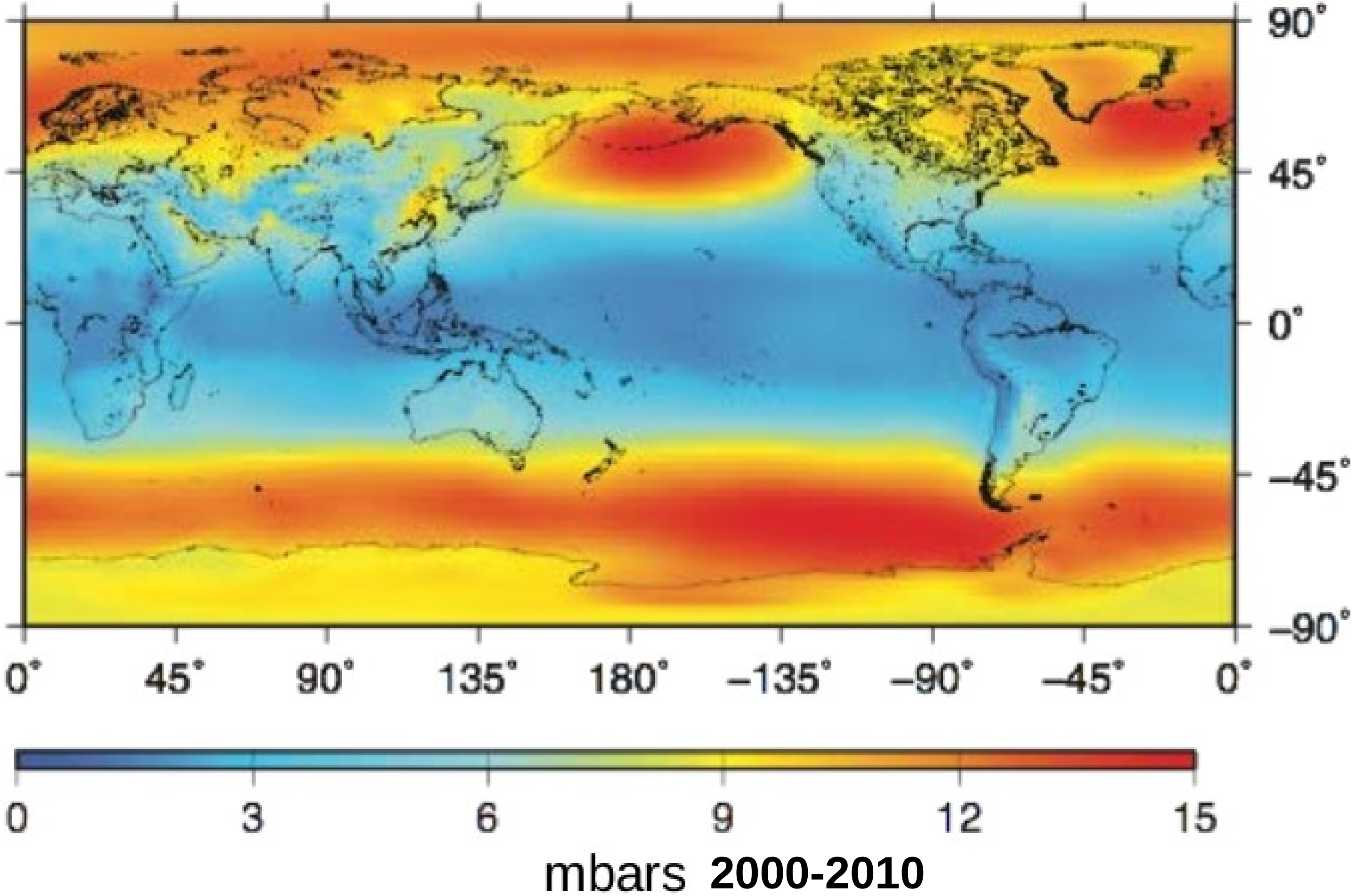

2000-2010

Largest changes close to poles

Lowest changes along the equator due to small variability in the solar energy

vertical displacement RMS

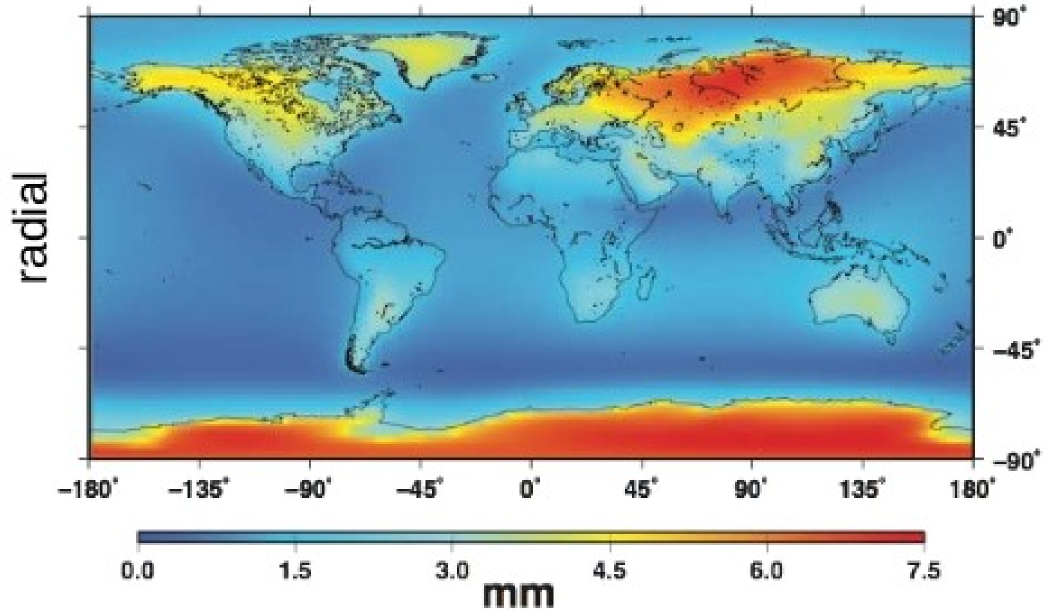

horizontal displacement

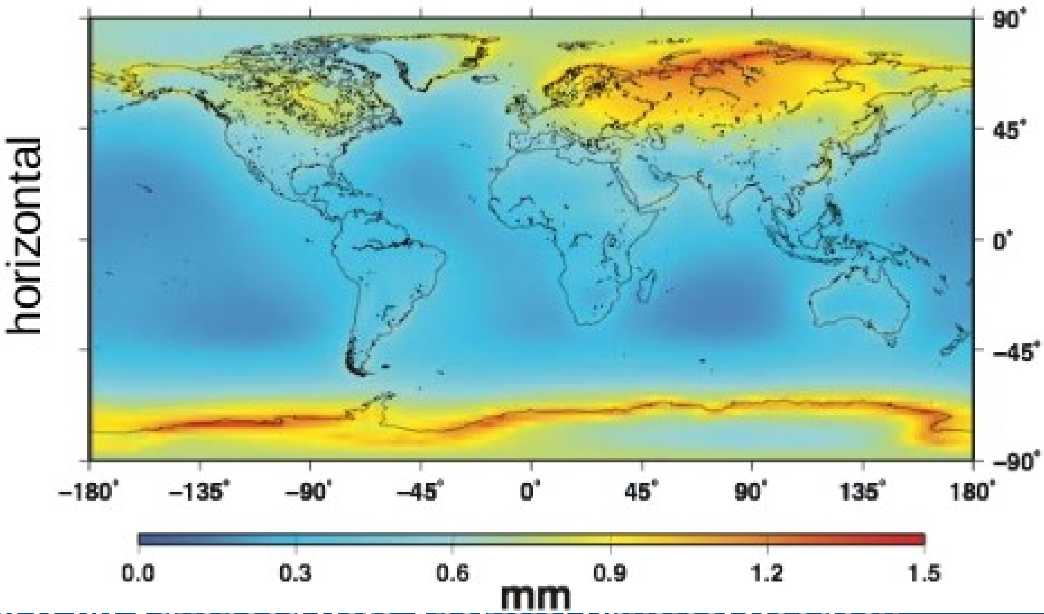

*** Larger variability at mid-lat to high-lat**

*** Horizontal displacement is 5 times smaller than the vertical displacement**

***Coastal areas less affected by atmospheric loading due to the ocean response that tends to mitigate the effects of loading**

Where to look for atmospheric and oceanic loading data?

This paper gets you a nice overview!

Supplementary material to: Evidence of daily hydrological loading in GPS time series over Europe

Anne Springer · Makan A. Karegar · Jürgen Kusche · Jessica Keune · Wolfgang Kurtz · Stefan Kollet

the date of receipt and acceptance should be inserted later

Content

This file contains the following supporting information:

1. Removing outliers and offsets from GPS time series
2. Methodology of removing non-tidal atmospheric and oceanic loading deformation from GPS time series
3. Complementary results
4. Gridded total water storage estimates and full error covariance matrices from GRACE
5. Set up of the Community Land Model (CLM-3.5)
6. Assimilation of GRACE data into CLM3.5

ESMGFZ: three-hourly $0.5^\circ \times 0.5^\circ$ grid of non-tidal atmospheric and oceanic loading displacement models

ATMIB: three-hourly $0.5^\circ \times 0.5^\circ$ grid of non-tidal atmospheric loading displacement model

ERAin: six-hourly $0.5^\circ \times 0.5^\circ$ non-tidal atmospheric loading displacement model

ATMMO: six-hourly $0.5^\circ \times 0.5^\circ$ tailored non-tidal atmospheric and oceanic displacement model

ECCO2: daily $0.5^\circ \times 0.5^\circ$ non-tidal oceanic loading displacement model

Comparing Non-tidal oce and atm models with GPS over Europe

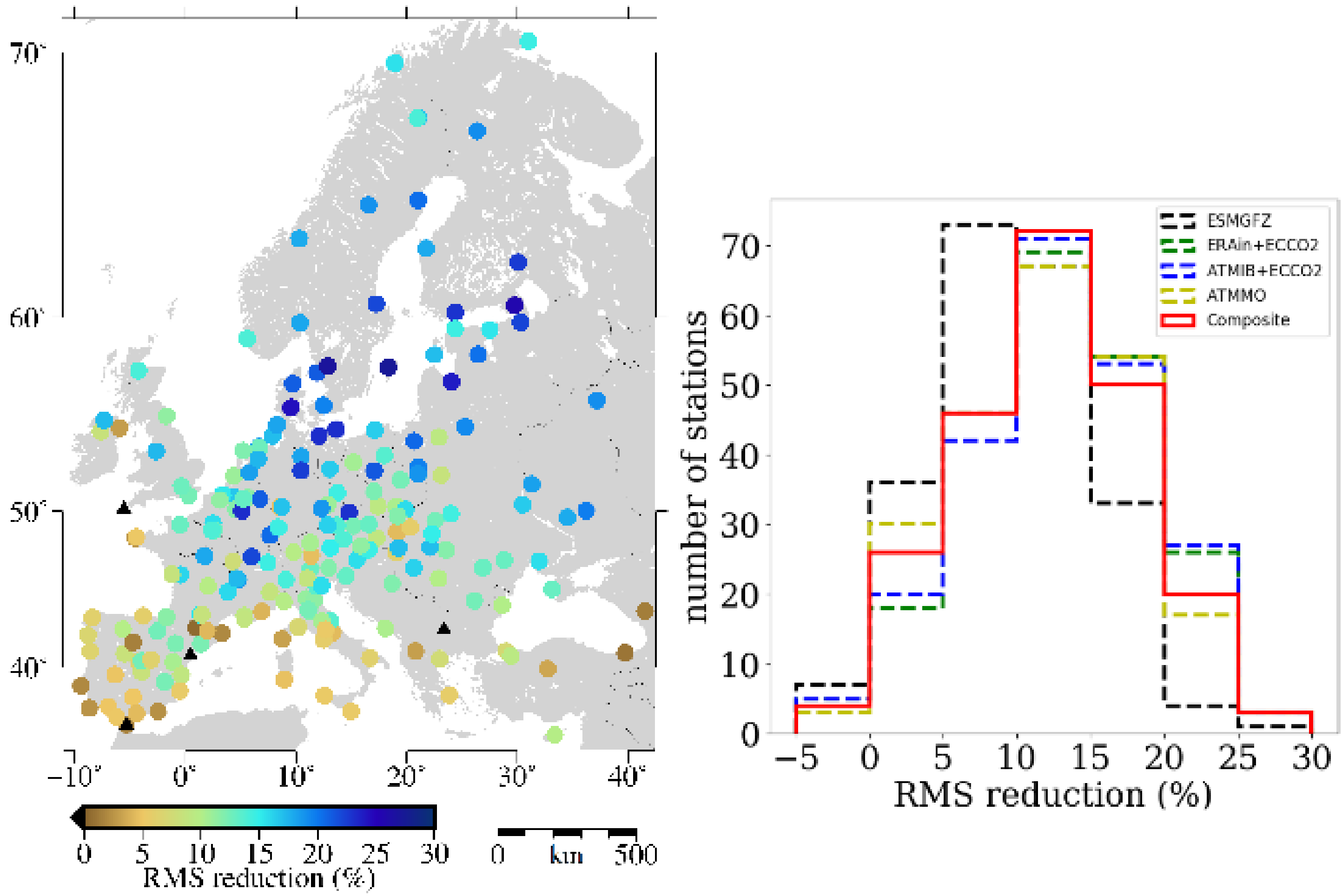

Fig. S1 (left) Reduction in scatter of GPS height time series (in percentage) after removing combined effects of non-tidal atmospheric and oceanic loading displacements using the composite model. The black triangles show stations where scatter of displacement time series become larger. (right) Histogram showing reduction in scatter of GPS height time series after removing combined effects of non-tidal atmospheric and oceanic loading displacements using different models.

Hydrological loading

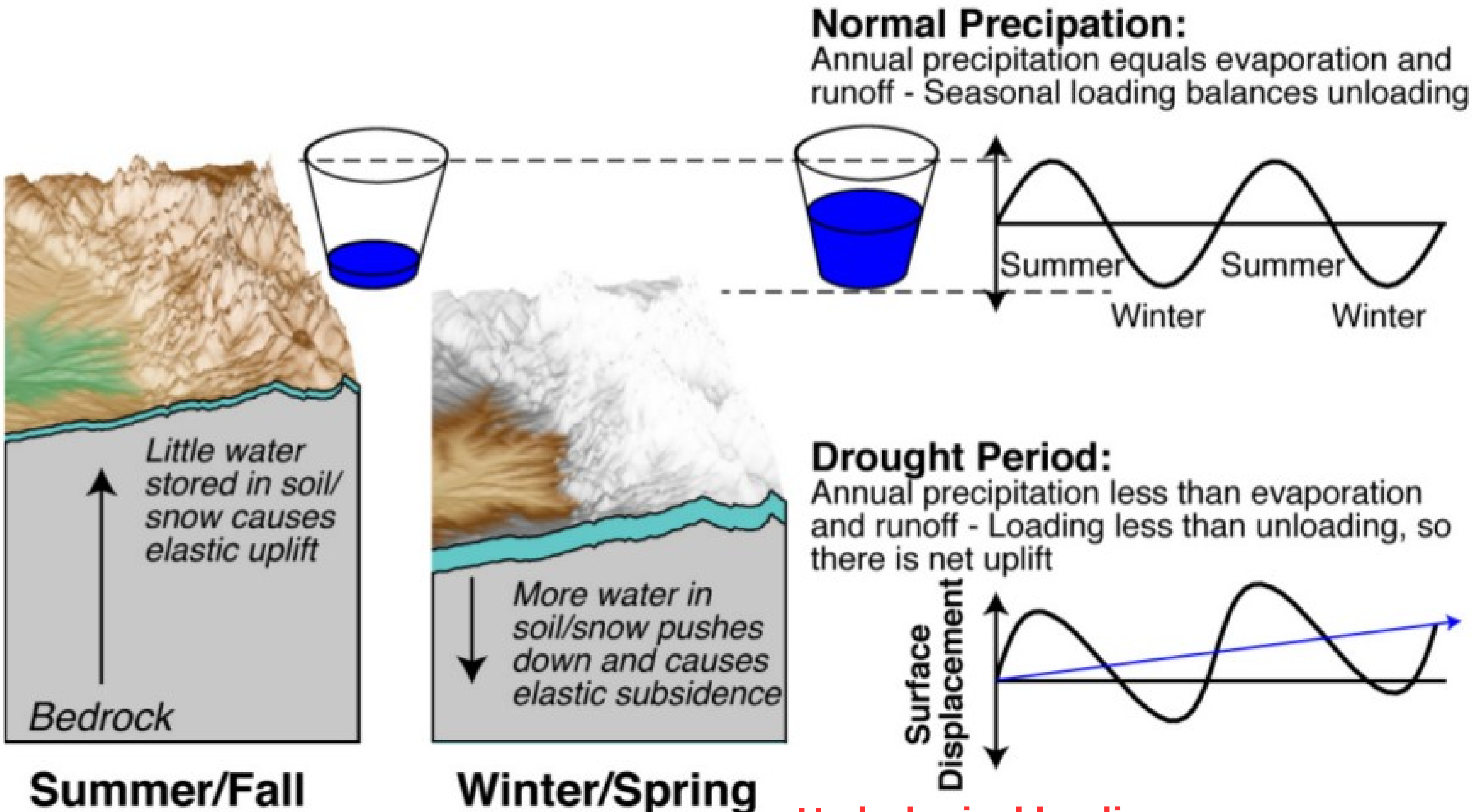

Source: UNAVCO

TWS

Hydrological loading:
* surface water: lakes, reservoirs and rivers
* groundwater
* snow pack and ice
* soil moisture
* vegetation

Poro-elastic effect:

Charge and recharge of aquifer could cause poro-elastic deformation: Think of opposite deformation of elastic loading

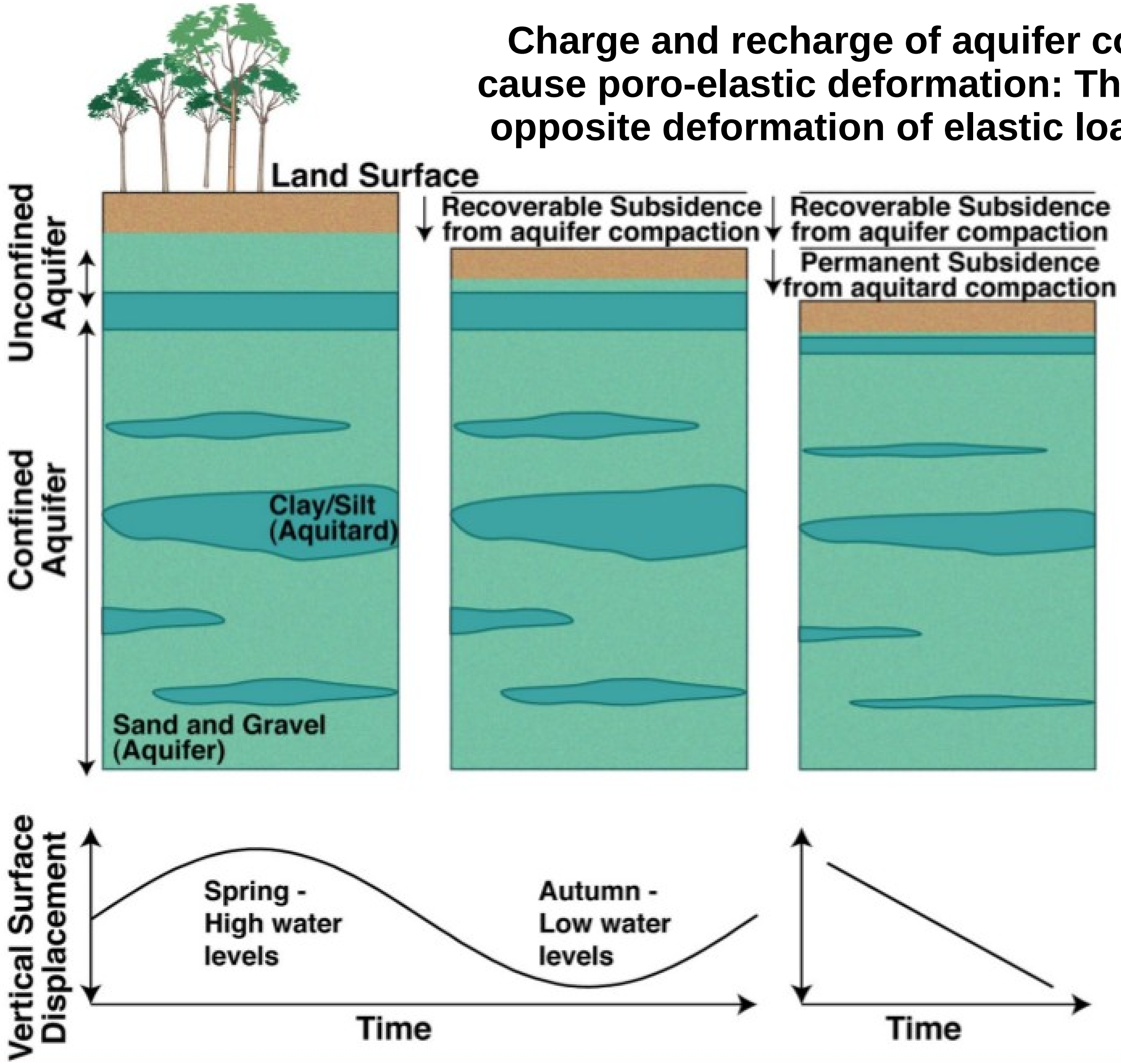

Source: UNAVCO

nature geoscience
LETTERS
PUBLISHED ONLINE: 16 MAY 2010 | DOI: 10.1038/NGEO845

Accelerating uplift in the North Atlantic region as an indicator of ice loss

Yan Jiang, Timothy H. Dixon* and Shimon Wdowinski

Vertical motions of the rocky margins of Greenland and Antarctica respond to mass changes of their respective ice sheets[1,2]. However, these motions can be obscured by episodes of glacial advance or retreat that occurred hundreds to thousands of years ago[3–6], which trigger a delayed response because of viscous flow in the underlying mantle. Here we present high-precision global positioning system (GPS) data that describe the vertical motion of the rocky margins of Greenland, Iceland and Svalbard. We focus on vertical accelerations rather than velocities to avoid the confounding effects of past events. Our data show an acceleration of uplift over the past decade that represents an essentially instantaneous, elastic response to the recent accelerated melting of ice throughout the North Atlantic region. Our comparison of the GPS data to models for glacial isostatic adjustment suggests that some parts of western coastal Greenland were experiencing accelerated melting of coastal ice by the late 1990s. Using a simple elastic model, we estimate that western Greenland's ice loss is accelerating at an average rate of 8.7 ± 3.5 Gt yr^{-2}, whereas the rate for southeastern Greenland—based on limited data—falls at 12.5±5.5 Gt yr^{-2}.

Inferring long-term trends from short-term measurements is challenging. For processes such as sea level rise or melting of

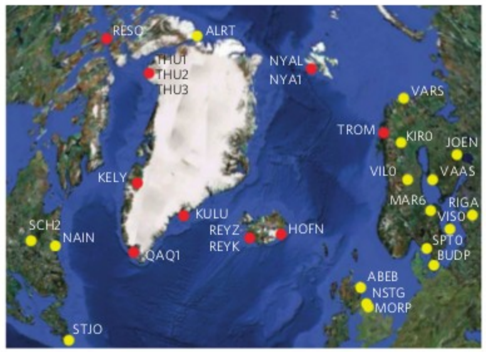

Figure 1 | Location of GPS sites used in this study. The red circles indicate sites with acceleration 0.5 mm yr^{-2} or greater; the yellow circles indicate acceleration less than this value.

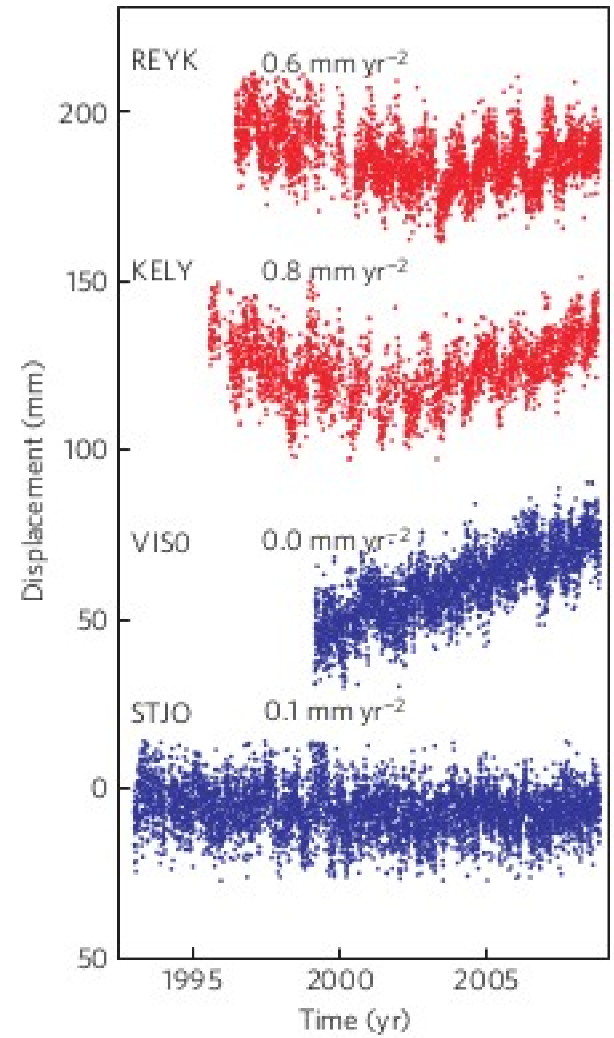

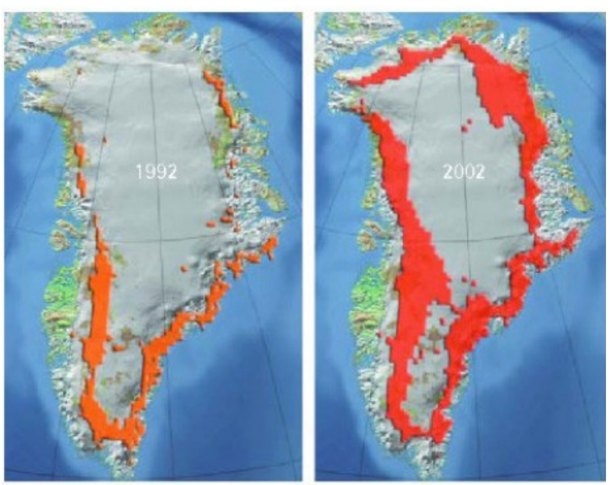

$$U(z=0) = \frac{(1-\nu)N_0}{\pi G(2a)} \times \left[2a + (x-a)\ln|x-a| - (x+a)\ln|x+a|\right] + \text{const}$$

River Loading in the Amazon: (Bevis et al. 2005)

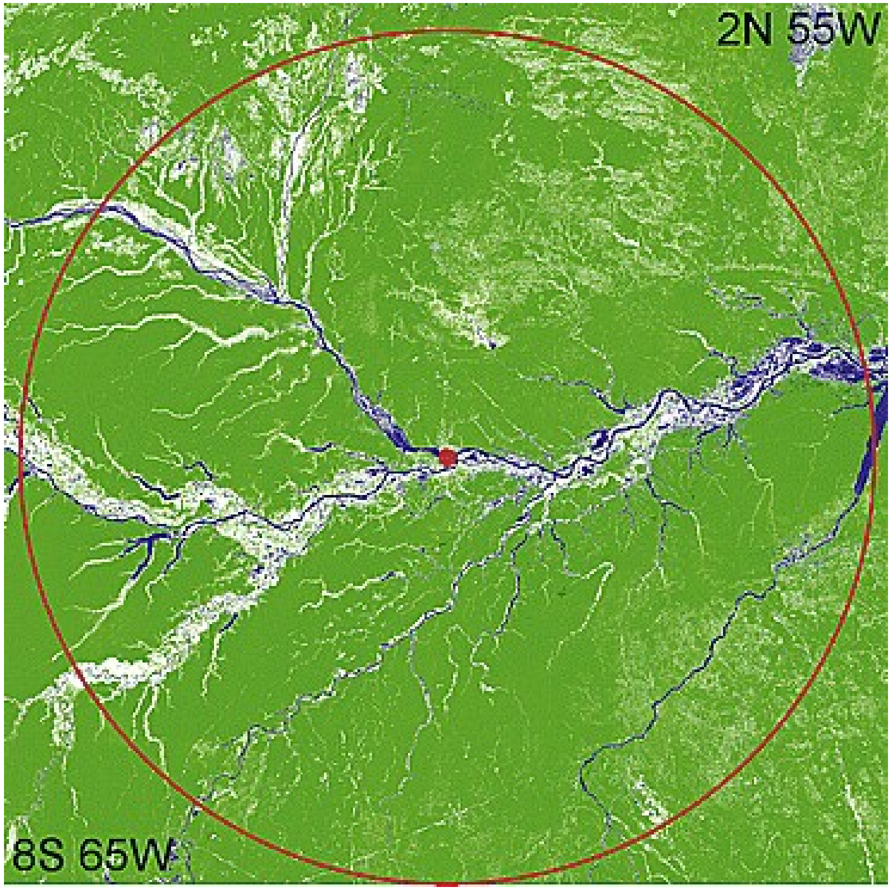

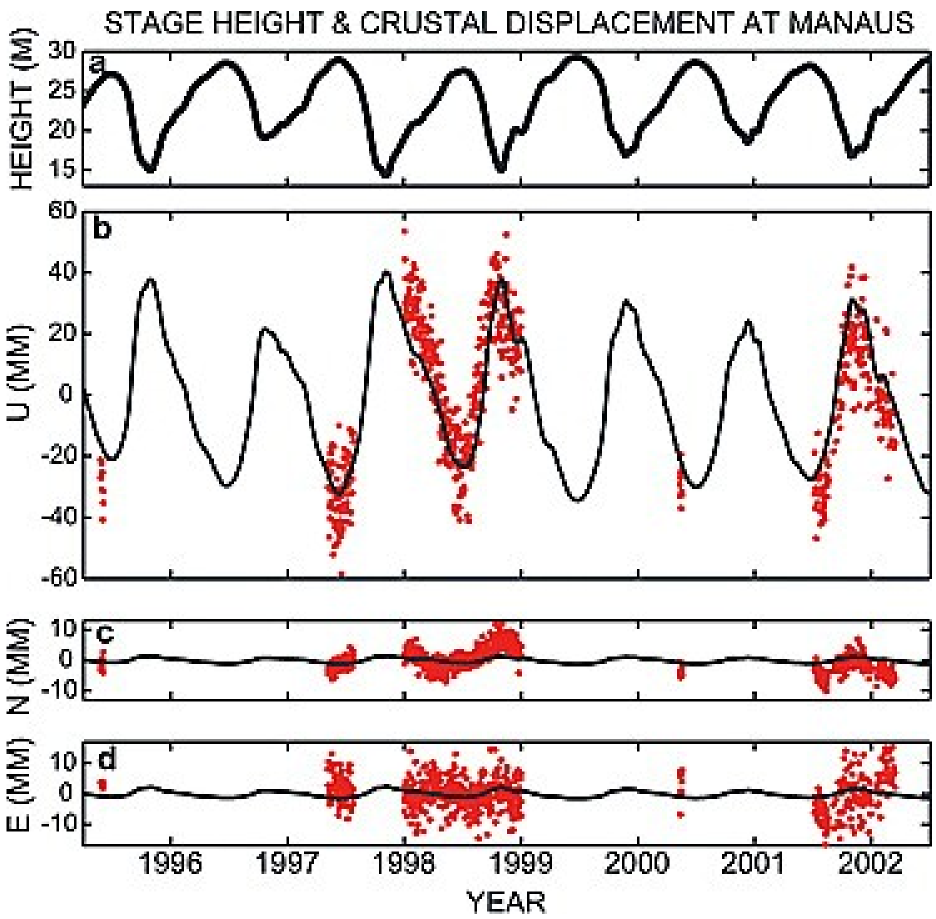

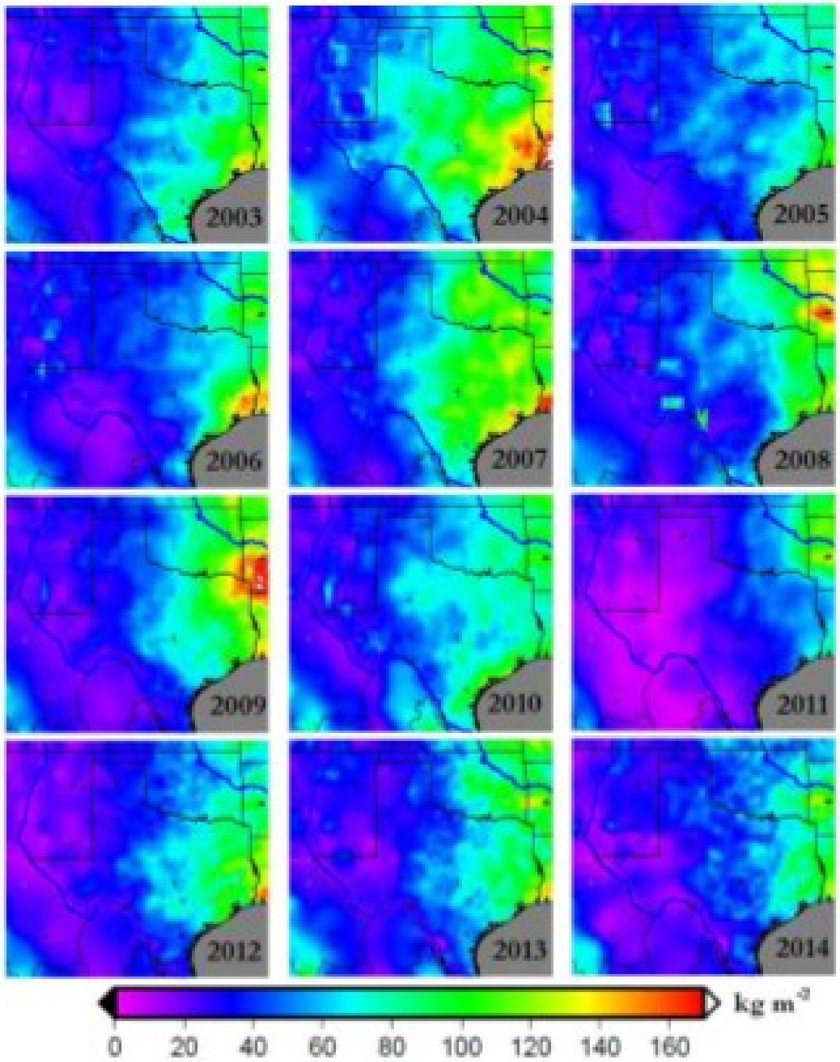

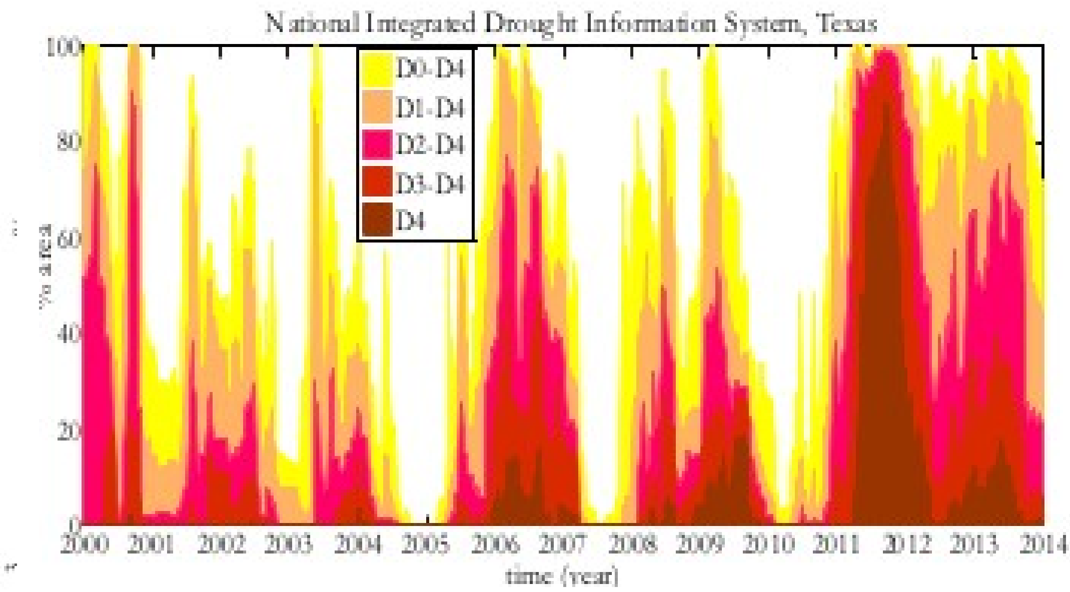

NLDAS mean annual rainfall

North American Land Data Assimilation System (NLDAS): hourly resolution at 0.125° grid

Data access: https://disc.gsfc.nasa.gov/datasets?keywords=NLDAS Karegar et al. (2014)

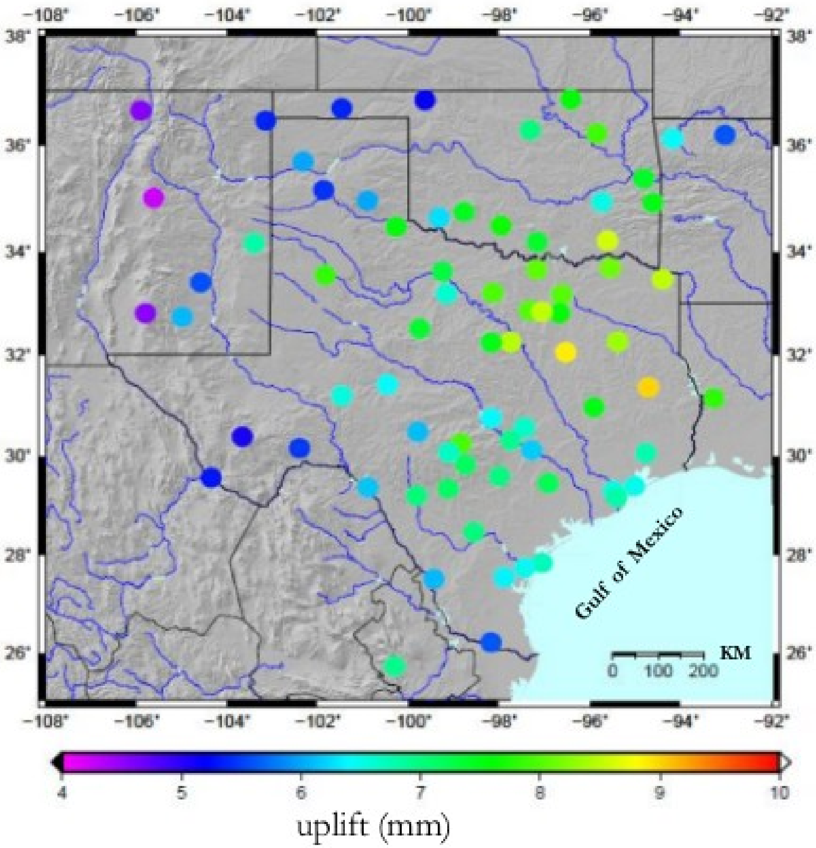

Uplift at GPS sites 2010-2012

Rectangular half-space model

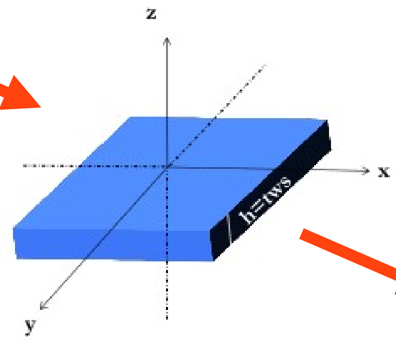

load = $\rho g h$

Total mass loss due to drought

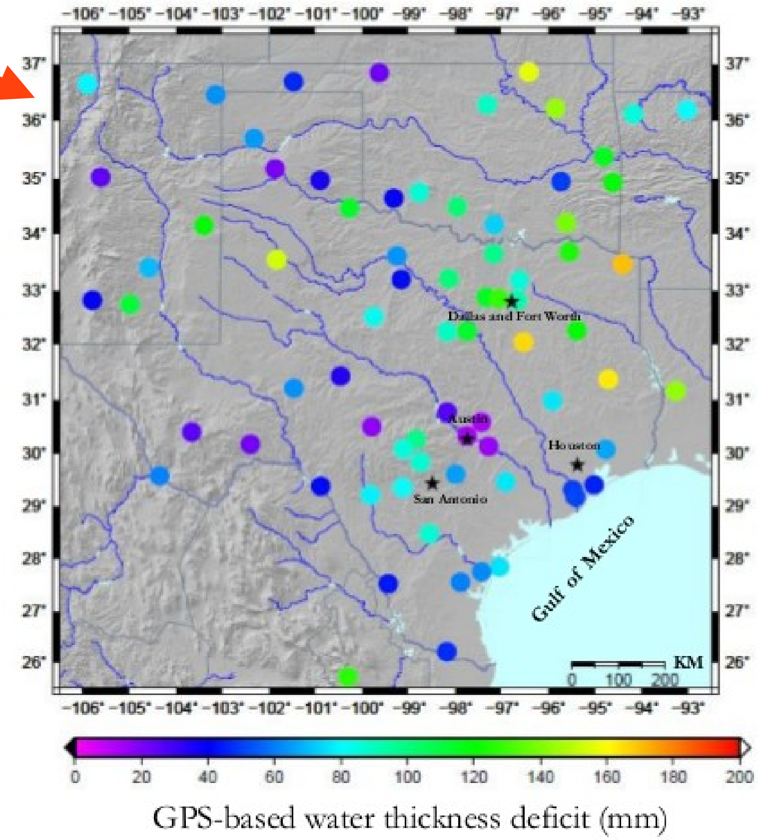

Karegar et al. (2014)

Half space model: Application to lakes and reservoirs and probing local structure of crust

Contents lists available at ScienceDirect

Earth and Planetary Science Letters

www.elsevier.com/locate/epsl

ELSEVIER

InSAR observations of lake loading at Yangzhuoyong Lake, Tibet: Constraints on crustal elasticity

CrossMark

Wenliang Zhao [a,*], Falk Amelung [a], Marie-Pierre Doin [b], Timothy H Dixon [c], Shimon Wdowinski [a], Guoqing Lin [a]

[a] Department of Marine Geosciences, Rosenstiel School of Marine and Atmospheric Science, University of Miami, 4600 Rickenbacker Causeway, Miami, FL 33149, USA
[b] ISTerre, CNRS, Univ. Joseph Fourier, Grenoble, France
[c] School of Geosciences, University of South Florida, Tampa, FL, USA

ARTICLE INFO

Article history:
Received 29 December 2015
Received in revised form 12 May 2016
Accepted 25 May 2016
Available online 17 June 2016
Editor: B. Buffett

Keywords:
InSAR time-series
surface loading
layered elastic half-space
Young's modulus
crustal elasticity

ABSTRACT

We use Envisat 2003–2010 InSAR imagery over Yangzhuoyong Lake in southeastern Tibet to study the elastic response of the Earth's crust to variations in lake level. The net lake level drop during our study period is ~3 m with seasonal variations of more than 1 m. The time-series close to the lake center shows a high correlation with the lake level history. Near the lake center the unit response with respect to lake level change is 2.5 mm/m in radar line-of-sight direction, or ~2.7 mm/yr in vertical direction, corresponding to a vertical response of ~4.3 mm/Gt load change. We show that the observations are most sensitive to the elastic properties of the crust in the 5–15 km depth range and explain them with a layered elastic half-space model with a Young's modulus of 50±9 GPa Young's modulus in the top 15 km of the crust and using moduli inferred from seismology at greater depth. The inferred Young's modulus is ~25% smaller than the seismic modulus, which we attribute to damaged rock and the presence of fluids.

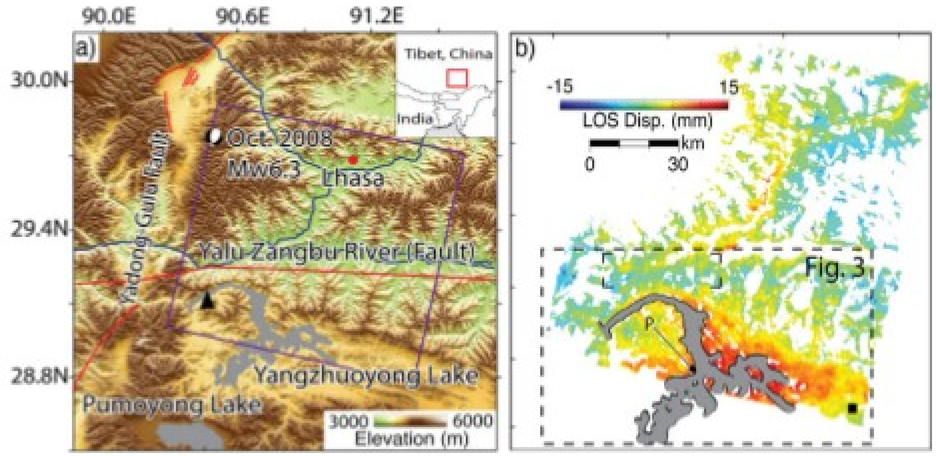

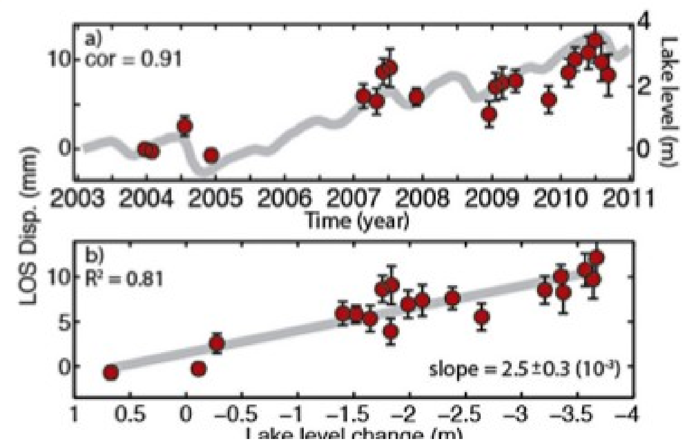

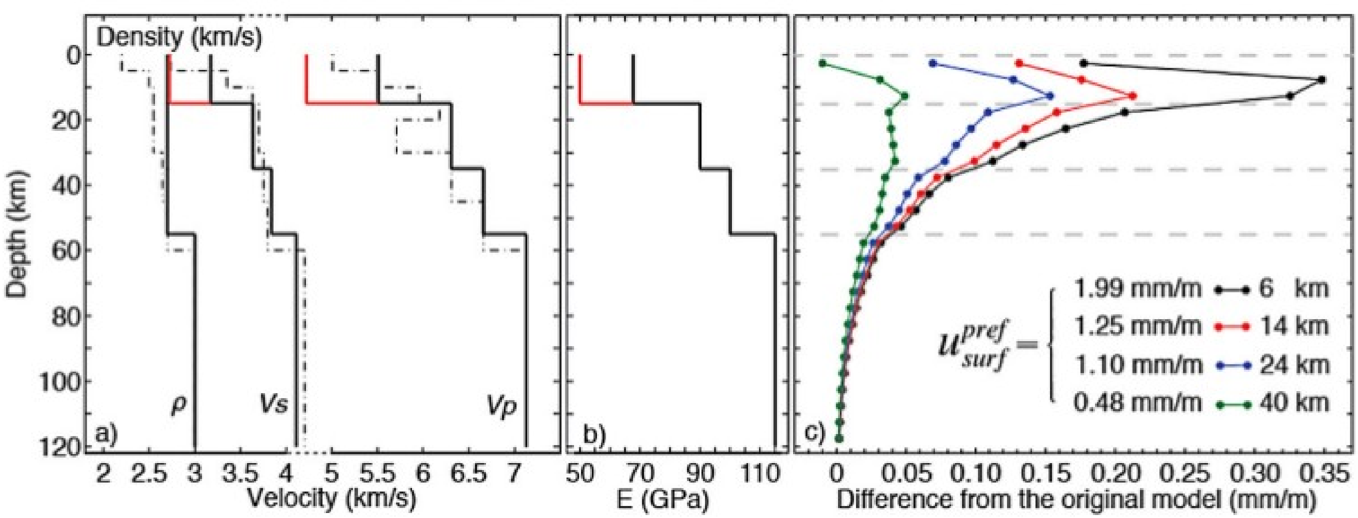

The elastic parameters are estimated by optimally fitting the modeled displacements to observed displacement (InSAR) through a half-space model and a given water load

TWS (m)

Cosine mode

From GPS

Sine mode

From a hydro model

Cosine mode

From GRACE

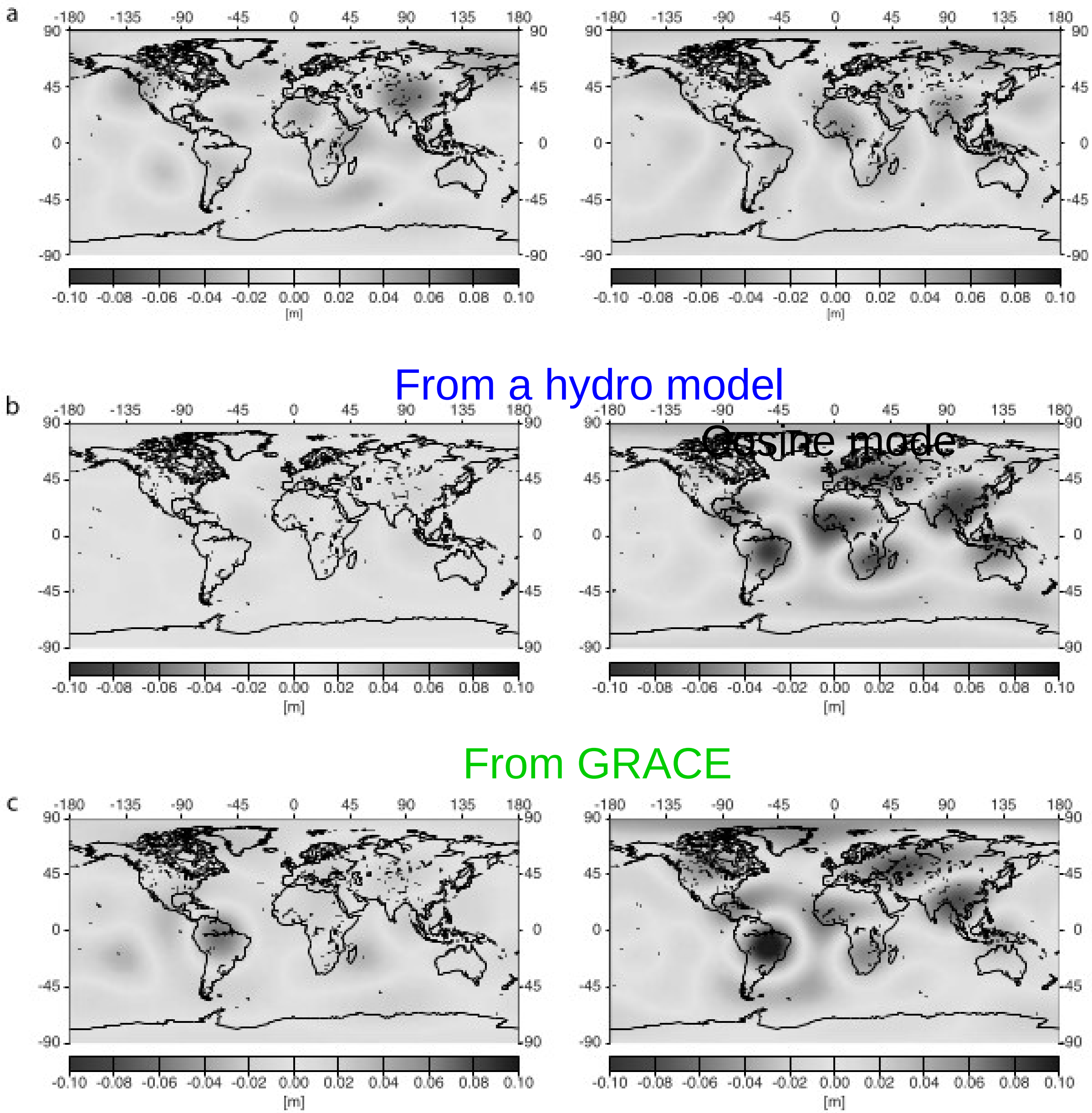

JOURNAL OF GEOPHYSICAL RESEARCH, VOL. 110, B09409, doi:10.1029/2004JB003556, 2005

Surface mass redistribution inversion from global GPS deformation and Gravity Recovery and Climate Experiment (GRACE) gravity data

J. Kusche and E. J. O. Schrama
Delft Institute of Earth Observation and Space Systems, Delft University of Technology, Delft, Netherlands

Received 29 November 2004; revised 15 April 2005; accepted 17 May 2005; published 20 September 2005.

[1] Monitoring hydrological redistributions through their integrated gravitational effect is the primary aim of the Gravity Recovery and Climate Experiment (GRACE) mission. Time-variable gravity data from GRACE can be uniquely inverted to hydrology, since mass transfers located at or near the Earth's surface are much larger on shorter timescales than those taking place within the deeper Earth and because one can remove the contribution of atmospheric masses from air pressure data. Yet it has been proposed that at larger scales this may be achieved independently by measuring and inverting the elastic loading associated with redistributing masses, e.g., with the global network of the International GPS Service (IGS). This is particularly interesting as long as GRACE monthly gravity solutions do not (yet) match the targeted baseline accuracies at the lower spherical harmonic degrees. In this contribution (1) we describe and investigate an inversion technique which can deal jointly with GPS data and monthly GRACE solutions. (2) Previous studies with GPS data have used least squares estimators and impose solution constraints through low-degree spherical harmonic series truncation. Here we introduce a physically motivated regularization method that guarantees a stable inversion up to higher degrees, while seeking to avoid spatial aliasing. (3) We apply this technique to GPS data provided by the IGS service covering recent years. We can show that after removing the contribution ascribed to atmospheric pressure loading, estimated annual variations of continental-scale mass redistribution exhibit pattern similar to those observed with GRACE and predicted by a global hydrology model, although systematic differences appear to be present. (4) We compute what the relative contribution of GRACE and GPS would be in a joint inversion: Using current error estimates, GPS could contribute with up to 60% to degree 2 till 4 spherical harmonic coefficients and up to 30% for higher-degree coefficients.

Hydrological loading: GLDAS model

GEOPHYSICAL RESEARCH LETTERS, VOL. 28, NO. 4, PAGES 651-654, FEBRUARY 15, 2001

Crustal displacements due to continental water loading

T. van Dam,[1] J. Wahr,[2] P. C. D. Milly,[3,4] A. B. Shmakin,[4,5] G. Blewitt,[6,7] D. Lavallée,[8] and K. M. Larson[9]

Abstract. The effects of long-wavelength (> 100 km), seasonal variability in continental water storage on vertical crustal motions are assessed. The modeled vertical displacements (Δr_M) have root-mean-square (RMS) values for 1994-1998 as large as 8 mm, with ranges up to 30 mm, and are predominantly annual in character. Regional strains are on the order of 20 nanostrain for tilt and 5 nanostrain for horizontal deformation. We compare Δr_M with observed Global Positioning System (GPS) heights (Δr_O) (which include adjustments to remove estimated effects of atmospheric pressure and annual tidal and non-tidal ocean loading) for 147 globally distributed sites. When the Δr_O time series are adjusted by Δr_M, their variances are reduced, on average, by an amount equal to the variance of the Δr_M. Of the Δr_O time series exhibiting a strong annual signal, more than half are found to have an annual harmonic that is in phase and of comparable amplitude with the annual harmonic in the Δr_M. The Δr_M time series exhibit long-period variations that could be mistaken for secular tectonic trends or post-glacial rebound when observed over a time span of a few years.

Introduction

The positioning time series from an individual GPS site predict vertical crustal motions due to long-wavelength (> 100 km) loading by continental water storage. We compare the modeled vertical surface displacements (Δr_M) with monthly height estimates from 147 globally distributed GPS sites. We also estimate the contribution of low-frequency variations in continental water loading to observed vertical displacement trends.

Calculation of continental water-storage loading and response

Storage of water in snowpack, soil, and groundwater was calculated using a global model of land water and energy balance, on a 1°-by-1°grid. The model is forced by estimated precipitation, downwelling radiation, and near-surface atmospheric conditions. Snowpack is tracked as a single store using mass- and energy-balance accounting. Snowmelt and rainfall recharge a single soil-water store until it is full (i.e., reaches field capacity), at which point any excess water recharges groundwater. Groundwater discharges to surface water at a rate proportional to groundwater storage, and surface-water storage changes are assumed negligible. Evaporation depletes snowpack at a rate determined by energy availability. Elsewhere, evaporation removes water from the

VERTICAL DISPLACEMENT RANGE
caused by total stored water/snow
Maximum - Minimum (1994-98)

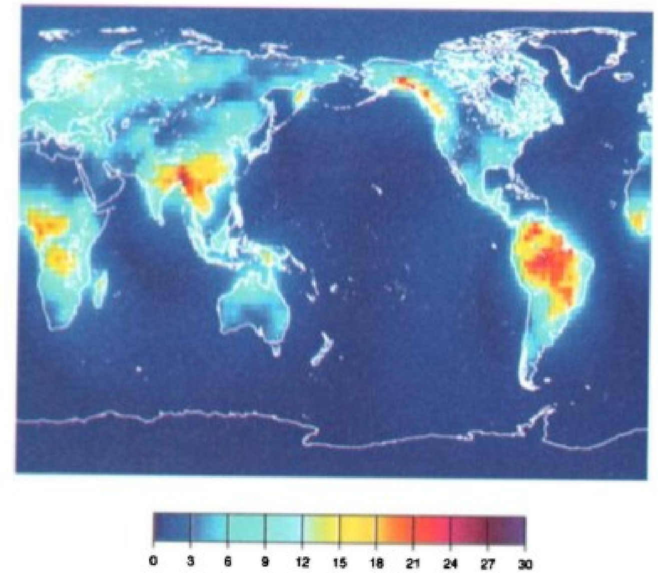

TRENDS 1996-1998

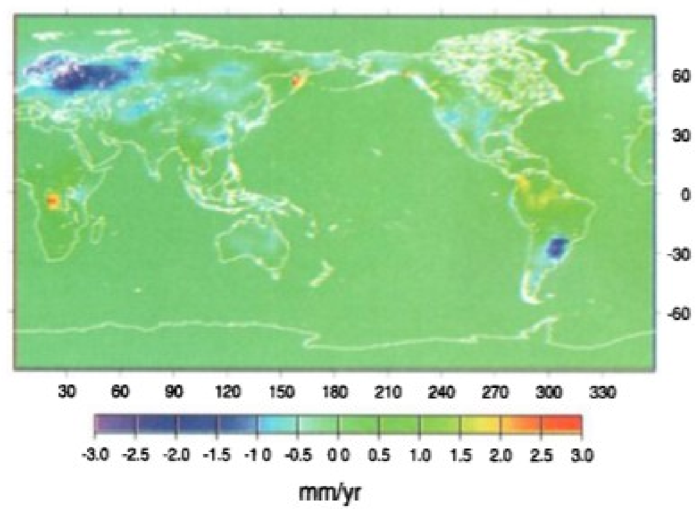

Global Land Data Assimilation System (GLDAS):

Hourly resolution and 0.25° grid

Data access:

https://disc.gsfc.nasa.gov/datasets?keywords=GLDAS

Hydrological loading: GRACE model

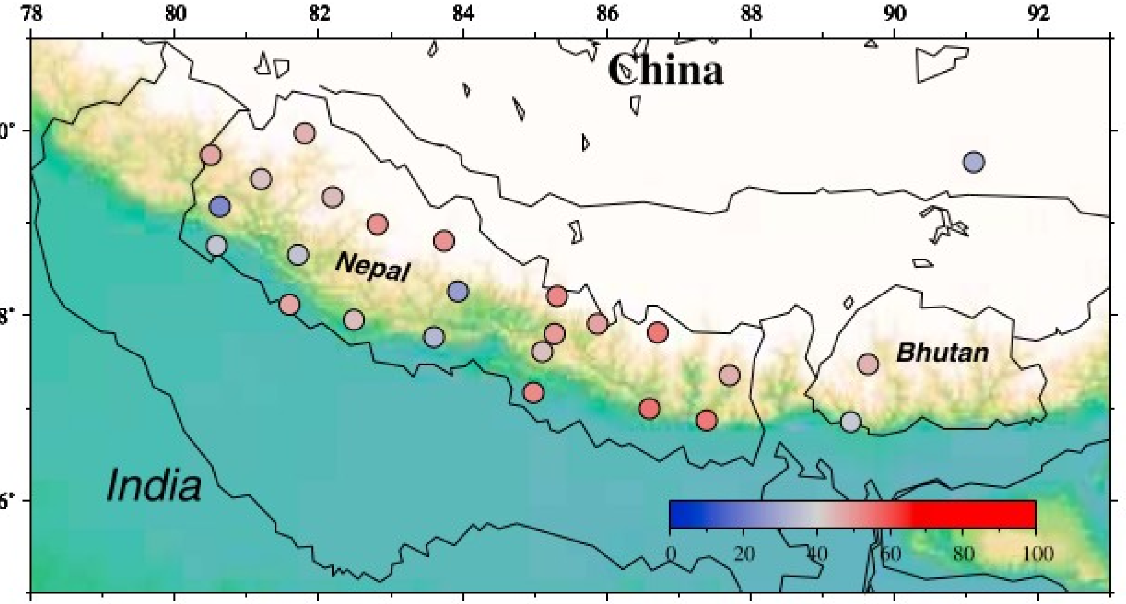

Figure 5. WRMS reductions for GPS detrended heights after removing GRACE-derived detrended displacements.

JOURNAL OF GEOPHYSICAL RESEARCH, VOL. 117, B03407, doi:10.1029/2011JB008925, 2012

Seasonal and long-term vertical deformation in the Nepal Himalaya constrained by GPS and GRACE measurements

Yuning Fu[1] and Jeffrey T. Freymueller[1]

Received 9 October 2011; revised 27 January 2012; accepted 30 January 2012; published 23 March 2012.

[1] We analyze continuous GPS measurements in Nepal, southern side of the Himalaya, and compare GPS results with GRACE observations in this area. We find both GPS and GRACE show significant seasonal variations. Further comparison indicates that the observed seasonal GPS height variation and GRACE-derived seasonal vertical displacement due to the changing hydrologic load exhibit very consistent results, for both amplitude and phase. For continuous GPS stations whose observation time span are longer than 3 years, the average WRMS reduction is ~45% when we subtract GRACE-derived vertical displacements from GPS observed time series. The comparison for annual amplitudes between GPS observed and GRACE-derived seasonal displacements also shows consistent correlation. The good seasonal correlation between GPS and GRACE is due to the improved GPS processing strategies and also because of the strong seasonal hydrological variations in Nepal. Besides the seasonal signal, GRACE also indicates a long-term mass loss in the Himalaya region, assuming no GIA effect. This mass loss therefore will lead to crustal uplift since the earth behaves as an elastic body. We model this effect and remove it from GPS observed vertical rates. With a 2D dislocation model, most GPS vertical rates, especially in the central part of Nepal, can be interpreted by interseismic strain from the Main Himalayan Thrust, and several exceptions may indicate the complexity of vertical motion in this region and some potential local effects.

Citation: Fu, Y., and J. T. Freymueller (2012), Seasonal and long-term vertical deformation in the Nepal Himalaya constrained by GPS and GRACE measurements, *J. Geophys. Res.*, *117*, B03407, doi:10.1029/2011JB008925.

$$RMS_{red} = \frac{rms(u_{GPS}) - rms(u_{GPS} - u_{model})}{rms(u_{GPS})} \times 100$$

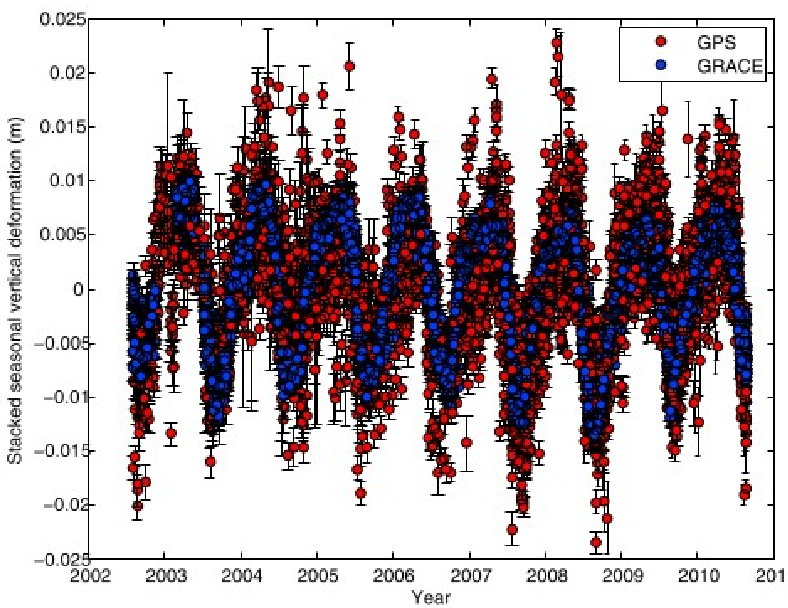

Figure 4. Stacked 10 day averaged GPS seasonal (detrended) vertical time series and GRACE-derived seasonal vertical time series, for the sites with data spans >3 years (see Table 1).

Data access:

Lecture 3

Hydrological loading: Combining GRACE and a hydro model

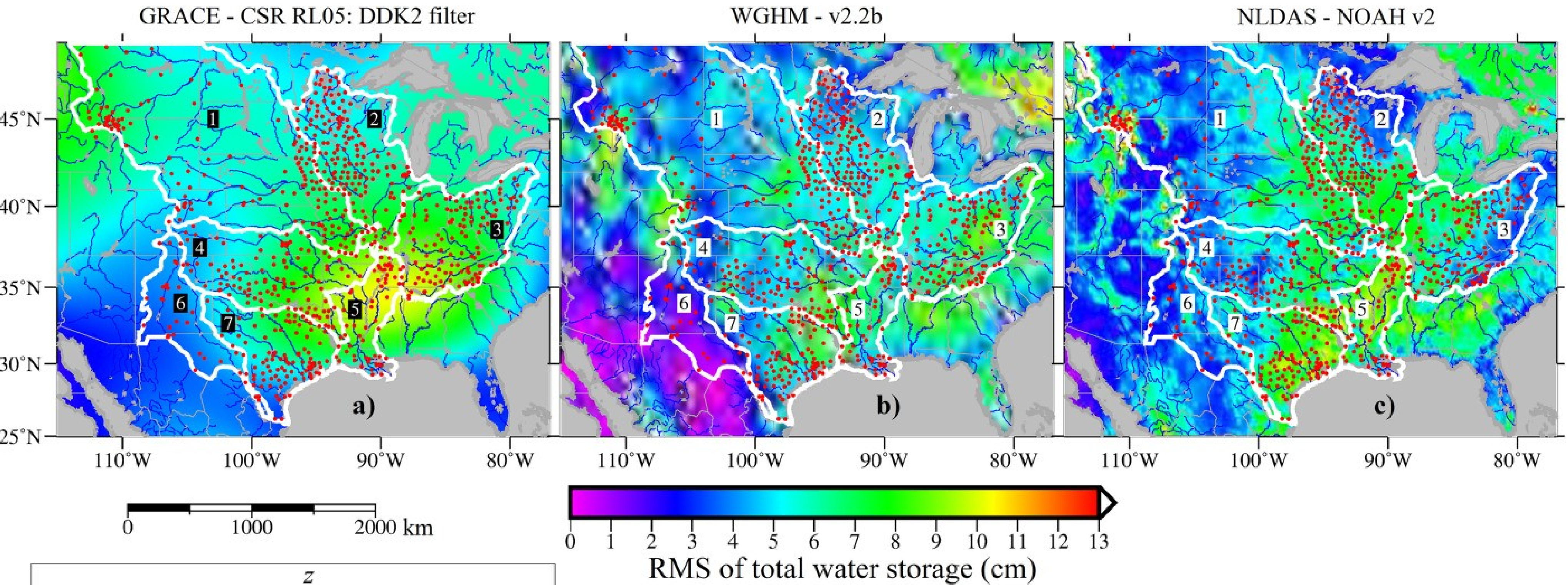

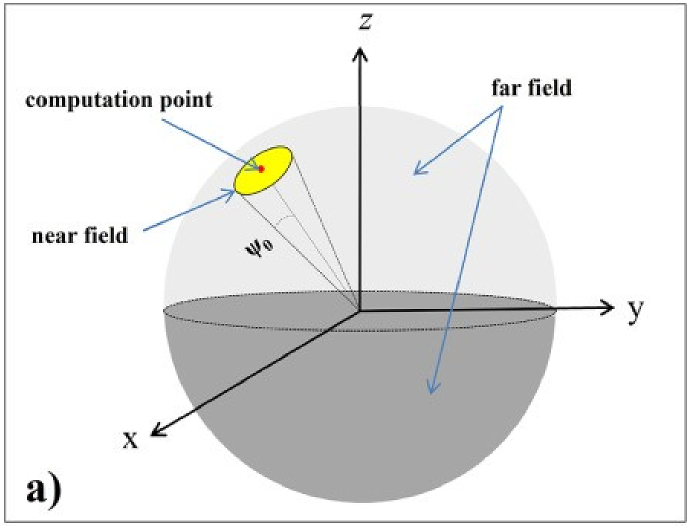

$$v(\theta,\ \lambda,\ t)=a^2 \iint_{\sigma} \Delta\sigma(\theta',\ \lambda',\ t)\ \ G(\psi)\ \ d\sigma$$

$$v(\theta,\ \lambda,\ t)=v_{nf}(\theta,\ \lambda,\ t)+v_{ff}(\theta,\ \lambda,\ t)$$

$$v_{ff}(\theta,\ \lambda,\ t)=\frac{a\rho_w}{2\rho_{avg}} \sum_{n=0}^{\infty} Q_n(\psi_0)\ \ \sigma_n(\theta, \lambda, t)$$

Karegar et al. (2018)

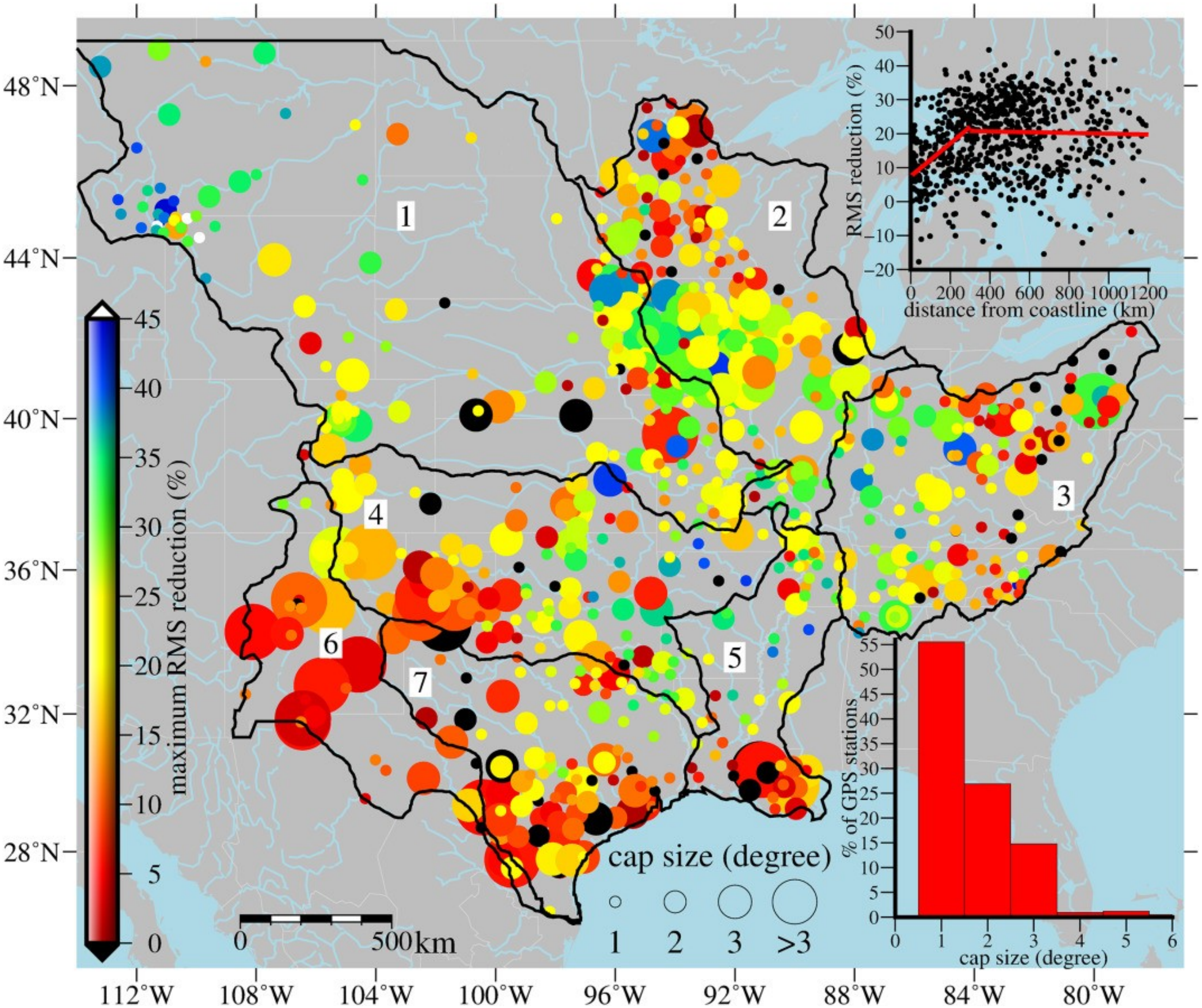

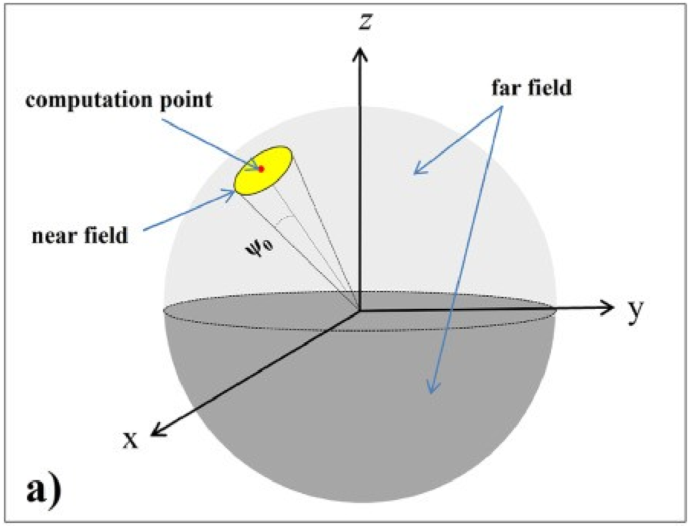

$$RMS_{red} = \frac{rms(u_{GPS}) - rms(u_{GPS} - u_{model})}{rms(u_{GPS})} \times 100$$

Karegar et al. (2018)

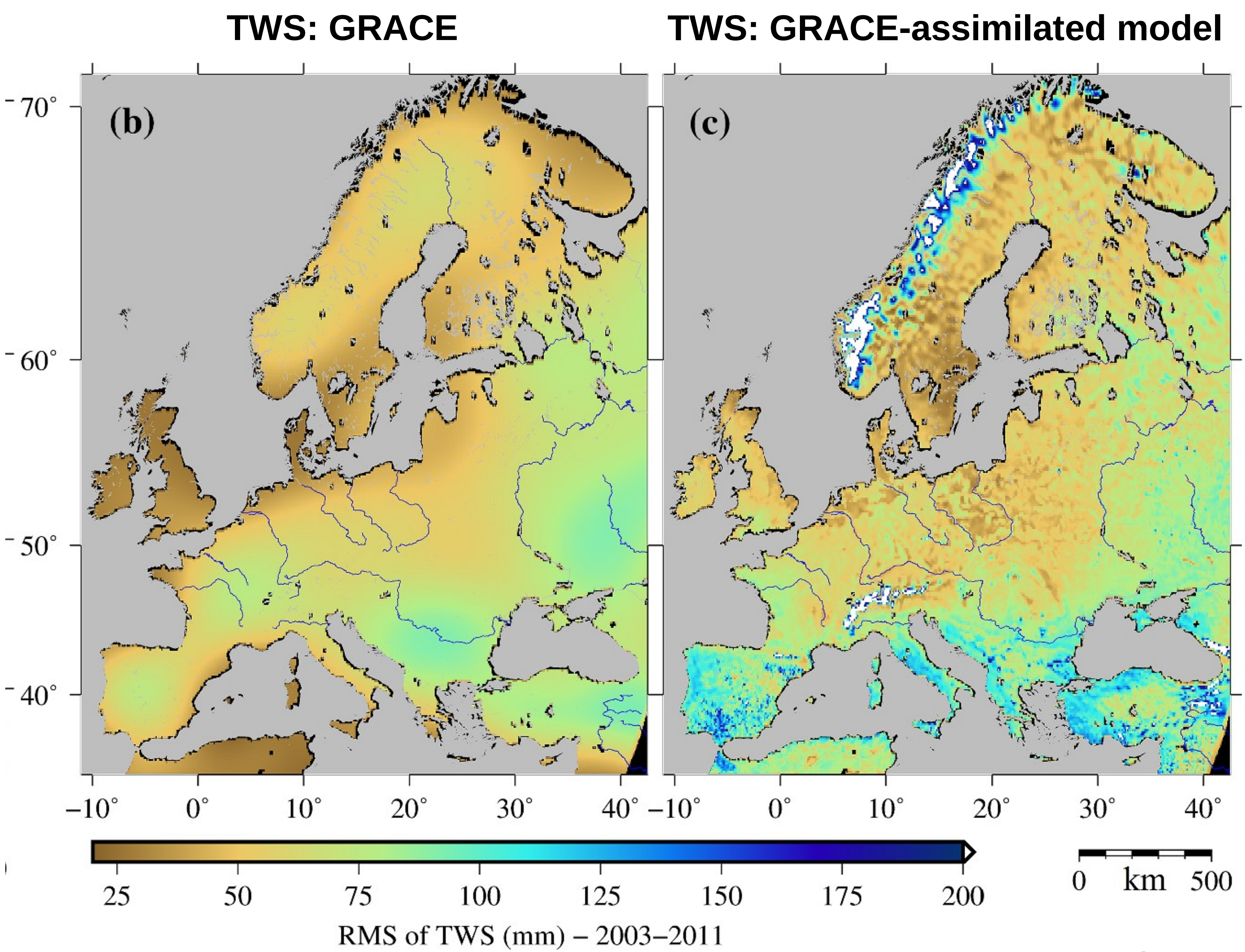

Springer et al. (2019)

What happens in spectra of loading data:

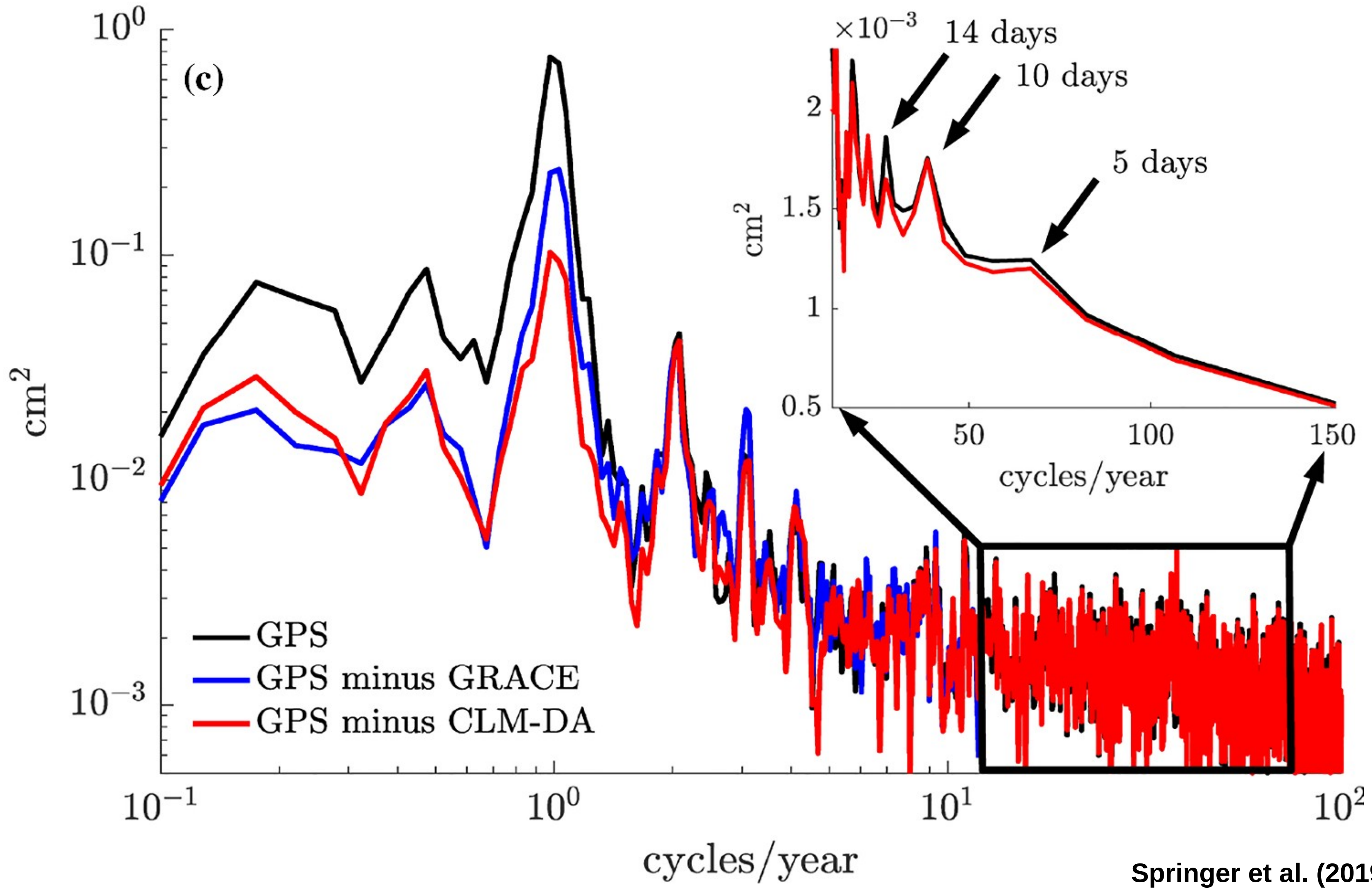

Springer et al. (2019)

Water load from rainfall caused up to 1 cm land subsidence.

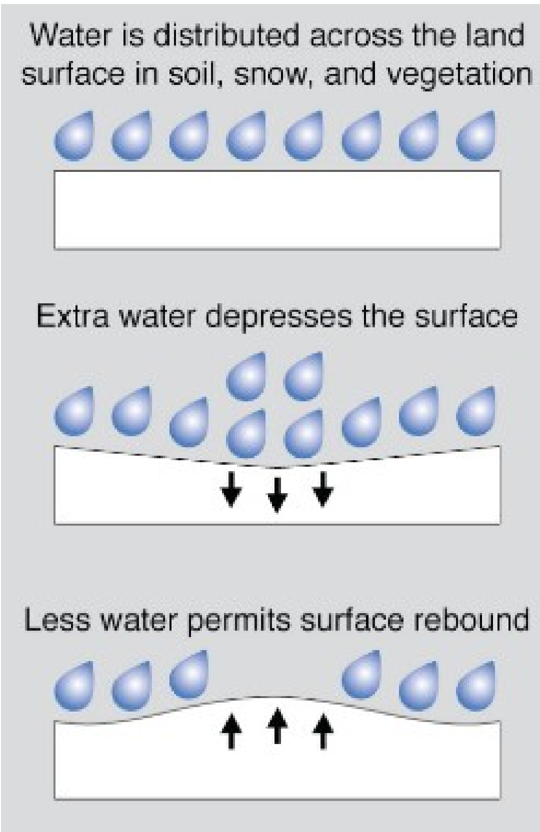

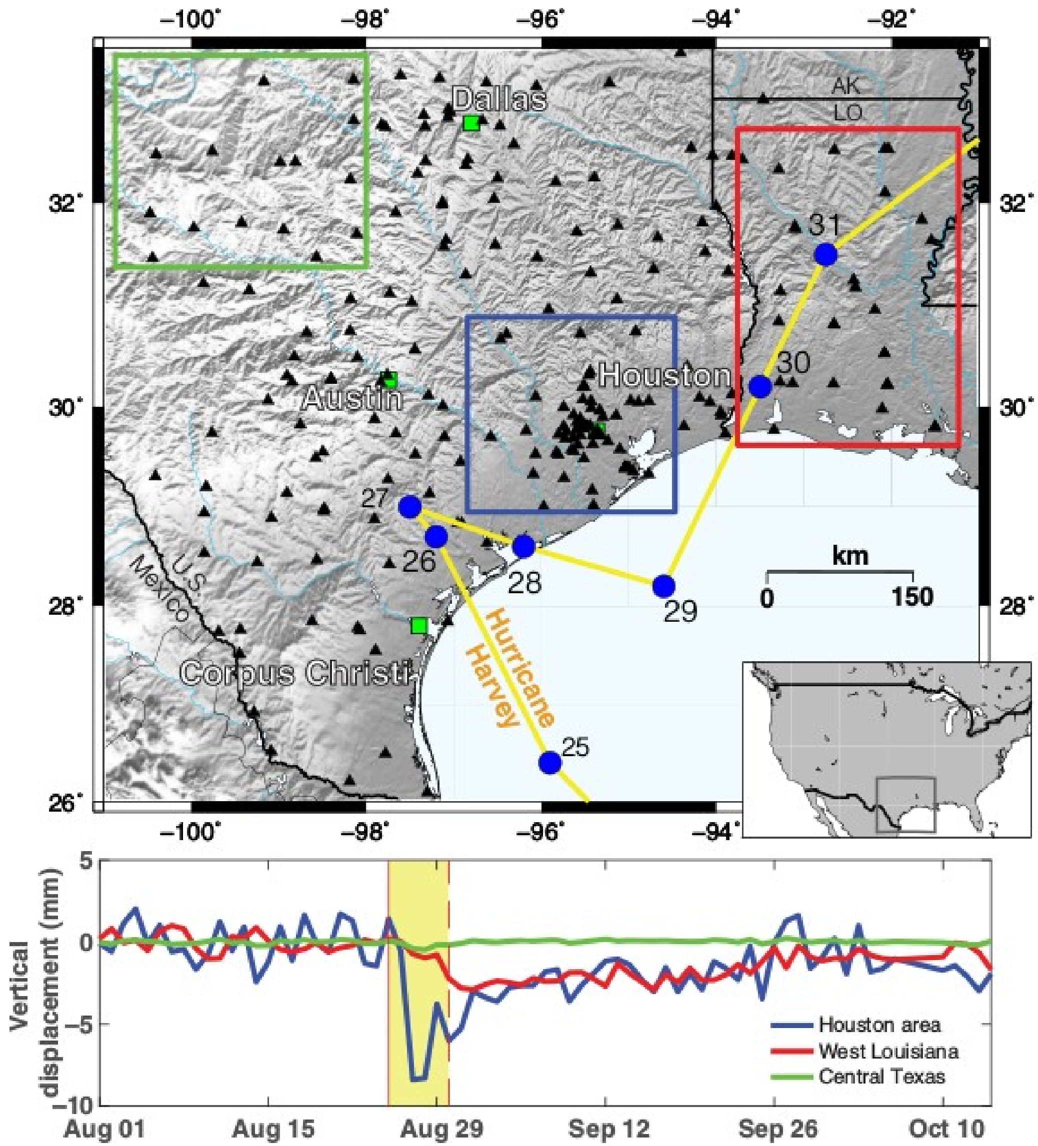

Milliner et al. (2018)

Land subsidence fro GPS is inverted to estimate the added mass from the rainfall

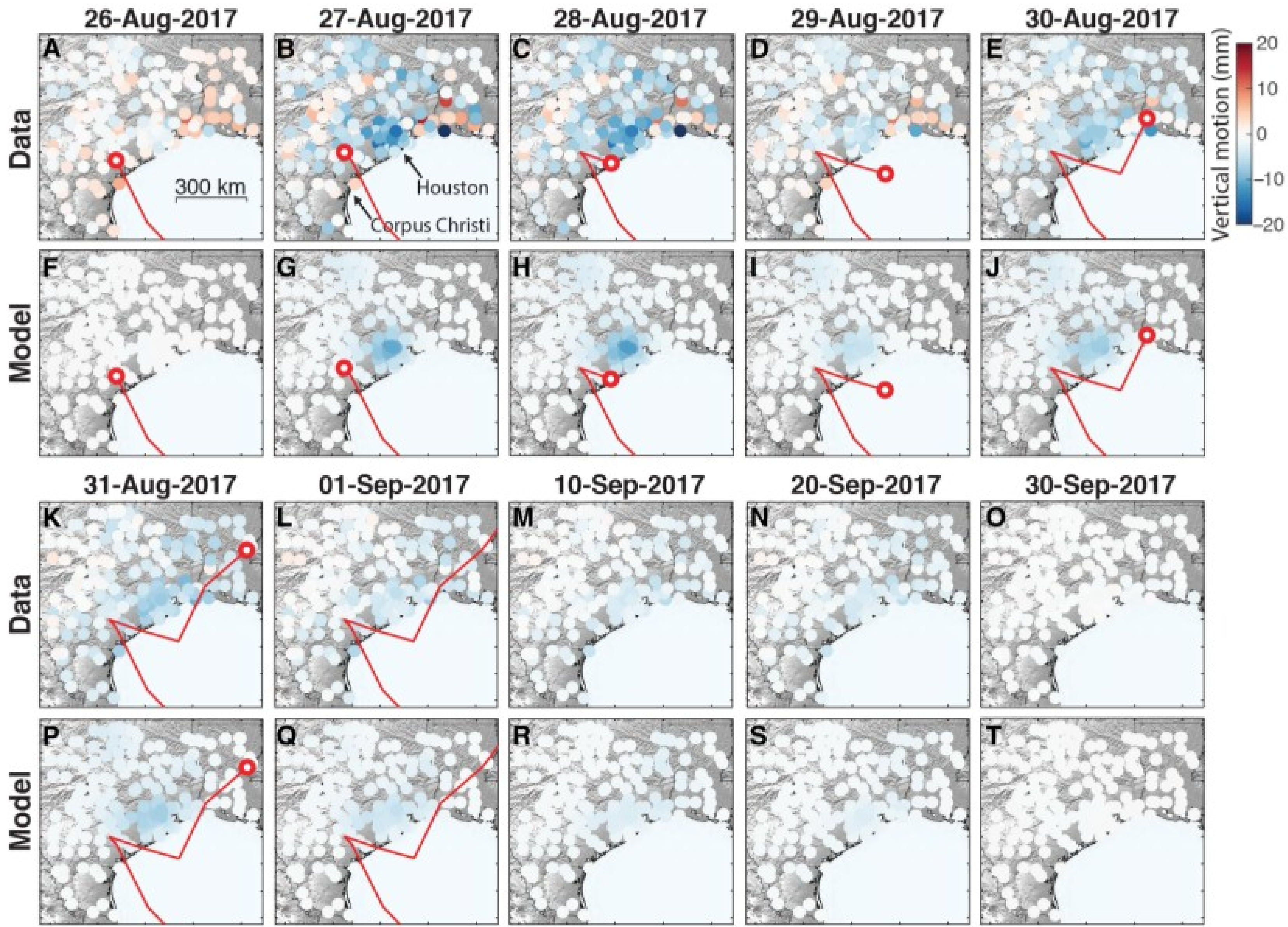

To what accuracy can we compute loading effects?

Earth tides / global (e.g. for satellite orbit computation) elastic Earth model / Love numbers are sufficient.

Earth tides / local (e.g. station motion, gravimeter) is well-known, local properties of the Earth model (high SH degrees) become important, could cause problems for precise measurements.

Loading effects at time scales up to years / decades: elastic Earth models if sufficient , but loading mass often not well-known!

Loading at longer time scales (postglacial rebound): viscoelastic Earth rheology not well-known, loads not well-known, this is often a big problem.